Pergamon

Neuropharmacology 43 (2002) 530–549

NEURO PHARMACOLOGY

www.elsevier.com/locate/neuropharm

# Ectopic expression of the $GABA_A$ receptor α6 subunit in hippocampal pyramidal neurons produces extrasynaptic receptors and an increased tonic inhibition

W. Wisden [a,*], D. Cope [b], T. Klausberger [b], B. Hauer [c], S.T. Sinkkonen [d], V. Tretter [c,1], R. Lujan [b,2], A. Jones [e], E.R. Korpi [d], I. Mody [f], W. Sieghart [c], P. Somogyi [b]

[a] *Department of Clinical Neurobiology, University of Heidelberg, Im Neuenheimer Feld 364, D-69120 Heidelberg, Germany*
[b] *MRC Anatomical Neuropharmacology Unit, Department of Pharmacology, Oxford University, Mansfield Road, Oxford OX1 3TH, UK*
[c] *Section of Biochemical Psychiatry, University Clinic for Psychiatry and Brain Research Institute, Division of Biochemistry and Molecular Biology, University of Vienna, A-1090 Vienna, Austria*
[d] *Department of Pharmacology and Clinical Pharmacology, University of Turku, FIN-20520 Turku, Finland*
[e] *MRC Laboratory of Molecular Biology, Neurobiology Division, Hills Road, Cambridge CB2 2QH, UK*
[f] *Department of Neurology, UCLA School of Medicine, 710 Westwood Plaza, Los Angeles, CA 90095-1769, USA*

Received 21 May 2002; received in revised form 5 July 2002; accepted 16 July 2002

**Abstract**

We generated transgenic (Thy1α6) mice in which the $GABA_A$ receptor α6 subunit, whose expression is usually confined to granule cells of cerebellum and cochlear nuclei, is ectopically expressed under the control of the pan-neuronal Thy-1.2 promoter. Strong Thy1α6 subunit expression occurs, for example, in deep cerebellar nuclei, layer V isocortical and hippocampal pyramidal cells and dentate granule cells. Ligand binding and protein biochemistry show that most forebrain α6 subunits assemble as α6βγ2-type receptors, and some as α1α6βγ2 and α3α6βγ2 receptors. Electron microscopic immunogold labeling shows that most Thy1-derived α6 immunoreactivity is in the extrasynaptic plasma membrane of dendrites and spines in both layer V isocortical and CA1pyramidal cells. Synaptic immunolabeling is rare. Consistent with the α6 subunits' extrasynaptic localization, Thy1α6 CA1 pyramidal neurons have a five-fold increased tonic $GABA_A$ receptor-mediated current compared with wild-type cells; however, the spontaneous IPSC frequency and the mIPSC amplitude in Thy1α6 mice decrease 37 and 30%, respectively compared with wild-type. Our results strengthen the idea that $GABA_A$ receptors containing α6 subunits can function as extrasynaptic receptors responsible for tonic inhibition and further suggest that a homeostatic mechanism might operate, whereby increased tonic inhibition causes a compensatory decrease in synaptic $GABA_A$ receptor responses.


*Keywords:* Thy-1.2 gene promoter; Transgenic mice; Extrasynaptic receptor; Tonic inhibition; Cerebral cortex; Cerebellum

## 1. Introduction

$GABA_A$ receptors participate in two modes of inhibition: first, fast point-to-point synaptic transmission via the simultaneous opening of synaptic $GABA_A$ receptors resulting in inhibitory postsynaptic currents (IPSCs—phasic inhibition); and second, the diffusion of GABA away from the synapse to activate extrasynaptic receptors. Activation of extrasynaptic receptors produces a constant inhibitory current termed 'tonic inhibition', or 'spill over inhibition' if the GABA diffuses to and activates receptors on a distant cell (Rossi and Hamann, 1998; Mitchell and Silver, 2000). The locations (synaptic and extrasynaptic) and properties (e.g. desensitization rate; affinity) of the $GABA_A$ receptor subtypes on the cell are thus important determinants of the inhibitory response (Nusser et al., 1998; Mody, 2001; Wisden and Farrant, 2002).

* Corresponding author. Tel.: +49-6221-562403; fax: +49-6221-561397.
*E-mail address:* William.Wisden@urz.uni-heidelberg.de (W. Wisden).
[1] Present address: MRC LMCB and Department of Pharmacology, University College London, London WC1E 6BT, UK
[2] Present address: Centro Regional de Investigaciones Biomedicas, Facultad de Medicina, Universidad de Castilla-La Mancha, 02071 Albacete, Spain

0028-3908/02/$ - see front matter © 2002 Elsevier Science Ltd. All rights reserved.
PII: S0028-3908(02)00151-X

Tonic inhibition occurs in many brain regions (Ichinose and Lukasiewicz, 2002; Otis et al., 1991; Bai et al., 2001; Banks and Pearce, 2000), but has been particularly well studied for granule cells of the cerebellar cortex where incisive progress has been made (reviewed by Wisden and Farrant, 2002). GABA spillover from the Golgi cell to granule cell synapse results in a tonic inhibition by activating extrasynaptic receptors on the dendrites and cell soma (Kaneda et al., 1995; Tia et al., 1996; Brickley et al., 1996, 2001; Wall and Usowicz, 1997; Rossi and Hamann, 1998; Hamann et al., 2002). In fact, for granule cells, tonic inhibition provides threefold more inhibitory charge transfer than phasic inhibition through IPSCs (Brickley et al., 1996; Hamann et al., 2002). Distinct $GABA_A$ receptor subtypes carry the phasic and tonic currents. Receptors with a γ2 subunit, probably mainly α1βγ2 and α6βγ2 (and possibly α1α6βγ2) are synaptically located (Nusser et al., 1996a,b, 1998, 1999; Somogyi et al., 1996).

On cerebellar granule cells, GABA in the extracellular space outside the synaptic cleft is probably sensed mainly by α6βδ receptors as deduced from the following observations: the δ subunit is located exclusively extrasynaptically (Nusser et al., 1998); the δ subunit partners solely with α6 (Jones et al., 1997; Nusser et al., 1999); selective pharmacological blockade shows that the receptors mediating spill over and tonic inhibition contain α6 subunits (Rossi and Hamann, 1998; Hamann et al., 2002); and in genetically engineered granule cells lacking the α6 and δ subunits, the tonic inhibition is abolished (Brickley et al., 2001). Furthermore, dentate gyrus and cerebellar granule cells from mice lacking the δ subunit have no tonic $GABA_A$-receptor mediated current (Stell, Brickley, Farrant, Tang and Mody, unpublished), even though the cerebellar granule cells in δ −/− mice express more α6βγ2 receptors (Tretter et al., 2001), thus indicating the requirement for α6βδ rather than α6βγ2 receptors. Matching with their suggested in vivo function, recombinant α6βδ-type $GABA_A$ receptors have a high affinity for GABA and desensitize only slowly if GABA is continuously applied at low concentrations: EC50 for GABA is 0.2 μM for α6βδ, compared with 2 μM for α6β2γ2 and 10 μM for α1β2γ2 (Saxena and Macdonald, 1996; Haas and Macdonald, 1999; Hevers et al., 2000). It is important to note that all of the synaptic $GABA_A$ receptor subtypes on cerebellar granule cells (such as α6βγ2, α1βγ2 and α1α6βγ2) are also extrasynaptic, and so could in principle contribute to tonic responses; in addition, analysis of single channel conductance on granule cell patches indicates extrasynaptic (but not synaptic) receptors containing only α and β subunits (Brickley et al., 1999). Granule cells with no α1 subunit have a normal GABAergic tonic current (Vicini et al., 2001), ruling out the importance of α1-containing receptors for tonic inhibition. Nevertheless, one cannot be too dogmatic: in the presence of benzodiazepines and low GABA concentrations, extrasynaptic α1-containing receptors could make a substantial contribution to the background current because these drugs increase the apparent receptor affinity for GABA (Bai et al., 2001; Leao et al., 2000). Furthermore, receptors in the synaptic junction may also contribute to baseline noise if activated by GABA released at distant synapses and diffusing into the synaptic cleft from the non-synaptic extracellular space.

Normally α6 gene expression is restricted to rhombic-lip derived cerebellar and cochlear nucleus granule cells (Lüddens et al., 1990; Wisden et al., 1992; Varecka et al., 1994; Campos et al., 2001; Fig. 1C). In previous work we generated mice with no functional α6 subunit (Jones et al., 1997; Korpi et al., 1999; Mellor et al., 2000; Brickley et al., 2001). However, ectopic expression of a gene product can sometimes be as revealing as loss of function studies. So to further test the roles of α6-containing $GABA_A$ receptors in synaptic transmission, we generated transgenic mice in which the α6 subunit is expressed in many neuronal types throughout the brain. Our results support the idea that $GABA_A$ receptors containing the α6 subunit can function as extrasynaptic receptors responsible for tonic inhibition.

## 2. Methods

All animal experiments and associated procedures were in accordance with the UK Animals (Scientific Procedure) Act 1986 and the guidelines of the UCLA Chancellors Animal Research Committee.

### *2.1. Generation of Thy1α6 transgenic mice*

The mouse full-length $GABA_A$ receptor α6 subunit cDNA used for transgene construction was a gift from Stephen Moss (MRC LMCB and Department of Pharmacology, UCL, London, UK); the cDNA encodes an α6 subunit with a flag-epitope DYKDDDDK placed at the N-terminus just after the signal peptide in the context MVLLLPWLFILLWNAQA∗QLEDEG-DYKDDDKNFYS…, where ∗ is the predicted signal peptide cleavage site. The Flagα6 cDNA was inserted, as a SalI (5′)–XhoI (3′) fragment, into the unique XhoI site of the mouse Thy-1.2 expression cassette (Caroni, 1997; Fig. 1). The Thy1α6 transgene, purified as a NotI–PvuI fragment (Fig. 1), was injected into mouse eggs (strain CBA/cba×C57BL/6) (Hogan et al., 1994). Two Thy1α6 founders were obtained and expanded into independent homozygous lines on a C57BL/6 background; genotyping was by southern blotting using a α6 cDNA probe and digesting tail genomic DNA with *Bam*HI. Only one line was used for detailed analysis.

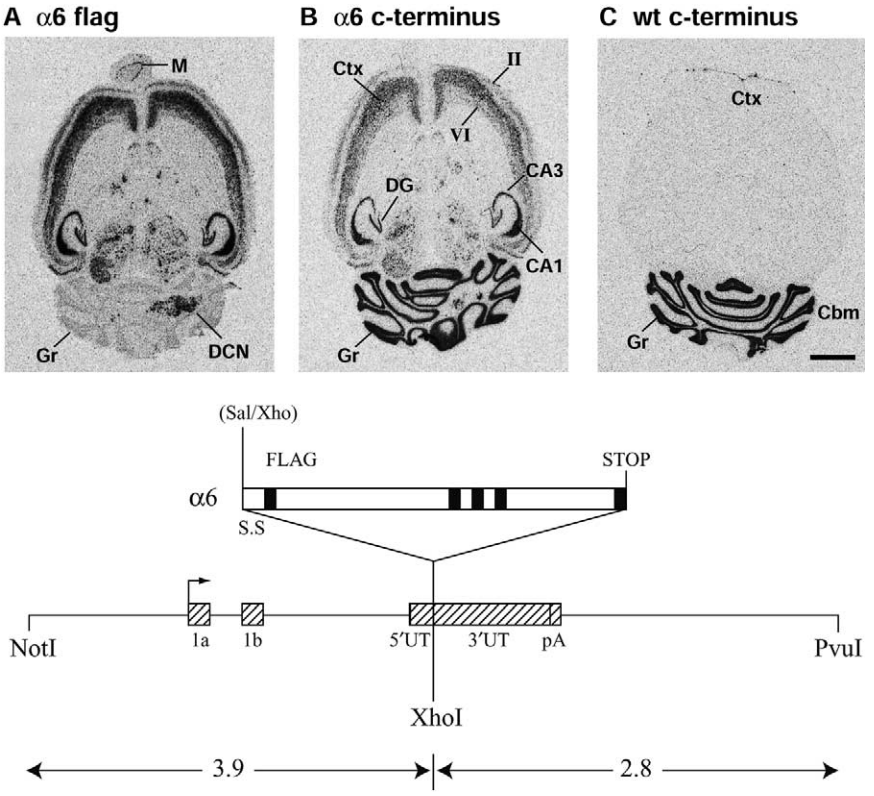


Fig. 1. Structure of the Thy1α6 transgene and its expression in adult Thy1α6 mouse brain as seen by in situ hybridization. Upper panel: in situ hybridization showing expression of the α6 transgenic mRNA in adult mouse brain as detected with $^{35}$S-labeled antisense oligonucleotide probes to the flag epitope (A) and with an α6-specifc probe recognizing both native and transgenic α6 mRNA (B and C). Panel C is the α6 gene expression in a wild-type mouse brain. Images are X-ray film autoradiographs. Cbm: cerebellar cortex; Ctx: neocortex; DCN: deep cerebellar nuclei; DG: dentate granule cells; Gr: cerebellar granule cells; M: mitral cells. II, and VI, layers of neocortex. Scale bar, 2 mm. Lower panel: Thy1α6 transgene structure. Exons of the Thy-1.2 gene are hatched. Arrow at exon 1a is the transcription start site. 5′UT, 5′ untranslated region; 3′UT, 3′ untranslated region; pA: polyadenylation sequence; SS: signal peptide; the unlabeled boxes in the α6 segment are the putative transmembrane domains.

### 2.2. In situ hybridization

Transgenic mouse brain sections were hybridized with $^{35}$S-labeled mouse α6-specific oligonucleotides exactly as described (Wisden and Morris, 2002). After hybridization, sections were exposed to Biomax film (Kodak) for two weeks. Oligonucleotides were mα6Flag and mα6Pan. mα6Flag: 5′-ACT GAC ATT TTC AGA GTA GAA GTT CTT GTC ATC GTC GTC CTT GTA GTC-3′ (antisense to the chimeric peptide sequence: DYKDDDDKNFYSENVS, where DYKDDDDK is the flag epitope and NFYSENVS is from the mouse α6 subunit). This oligonucleotide is specific for transgenic α6 subunit mRNAs; it gives no signal on wild-type mouse brain sections (not shown). The mα6Pan oligonucleotide is antisense to the nucleotide stretch encoding the peptide sequence LSRTPILKSTPV in the TM3-TM4 intracellular loop region of the mouse α6 subunit, and was described previously (Jones et al., 1996). The mα6Pan oligonucleotide hybridizes to both native and transgenically derived α6 subunit mRNAs.

### 2.3. Immunohistochemistry

#### 2.3.1. Antibodies

Two rabbit affinity-purified polyclonal antibodies to the $GABA_A$ receptor α6 subunit were used. Antibody α6(1–15)#17/15 was raised to amino acid residues 1–15 of the mature rat α6 subunit conjugated to keyhole limpet haemocyanine, and was used for light microscopic immunofluorescence labeling. Antibody α6(317–371)#21/6 was raised to a fusion protein consisting of amino acid sequence 317–371 of the mature rat α6 subunit of the $GABA_A$ receptor, maltose-binding-protein and seven histidine residues. Antibodies were affinity-purified as described earlier (Jechlinger et al., 1998). The specificity of both antibodies to the α6 subunit was revealed by their specific staining of cerebellar granule cells and the absence of immunolabeling of other cells in immunofluorescence, pre-embedding immunoperoxidase and silver intensified gold labeling, as well as in postembedding immunogold reactions. In addition, no immunolabeling could be observed in α6 subunit −/− mice

(Jones et al., 1997), as tested in this study by immunofluorescence labeling.

*2.3.2. Preparation of animals and tissues*

Seven adult Thy1α6, two α6−/− (Jones et al., 1997) and three wild-type C57BL/6 mice (Charles River, UK) were anaesthetized with Sagatal (pentobarbitone sodium, 220 mg/kg i.p.) and perfused through the heart with 0.9% NaCl saline followed by fixative containing 4% paraformaldehyde, 0.05% glutaraldehyde, and 0.2% picric acid in 0.1 M phosphate buffer (PB) pH 7.4 for 10–15 min. After perfusion the brains were left in situ for 10–15 min, then they were removed from the skull. For immunofluorescence analysis, the brains were sectioned sagitally at 60-μm thickness on a Vibratome. For electron microscopic analysis, blocks from the dorsal hippocampus, the parietal isocortex and the cerebellum were dissected and washed in 0.1 M PB, followed by sectioning on a Vibratome at 500 μm (for postembedding reactions) or 60 μm thickness (for pre-embedding reactions) and washed in 0.1 M PB.

*2.3.3. Fluorescence labeling*

Three Thy1α6, two α6−/− and two wild-type C57BL/6 mice were used. Sections were pre-incubated (1 h) with 20% normal goat serum (NGS) in 0.05 M Tris–HCl pH 7.4 containing 0.9% NaCl (TBS) and 0.1% Triton X100, and subsequently incubated at 4 °C for two days with the α6(1–15)#17/15 antibodies in 1% NGS dissolved in TBS–Triton at a final protein concentration of 0.8 μg/ml. After washing, the sections were incubated in swine anti-rabbit IgG conjugated to horseradish peroxidase (HRP, product no. P.0399, DAKO, Ely, UK) diluted 1:100 in 1% NGS dissolved in TBS–Triton. Peroxidase was visualized with the Tyramide enhancement Fluorescein System (NEN TSA™, Life Science Products, Boston, MA, USA); the tyramide reagent was diluted 1:50. The sections were washed in TBS and mounted in Vectashield (Vector Labs, Burlingame, CA, USA).

*2.4. Pre-embedding light and electron microscopic immunocytochemistry*

Procedures were performed on brain sections of two Thy1α6 and two C57Bl6 mice as described earlier (Baude et al., 1993) with minor modifications. Briefly, sections were pre-incubated (1 h) with 20% NGS in 0.05 M Tris–HCl pH 7.4 containing 0.9% NaCl (TBS), and subsequently incubated with α6(317–371)#21/6 antibodies in 1% NGS–TBS at a final concentration of 1.2 μg/ml. Immunoperoxidase reactions were carried out using the avidin–biotin–HRP complex method (ABC, Elite kit, Vector). Pre-embedding immunogold reactions were performed using anti-rabbit IgG coupled to ultra small gold particles in a 1:100 dilution (Aurion, Wageningen, Netherlands). Gold particles were enhanced by silver amplification (Aurion, Wageningen, Netherlands) for 60 min. Sections were then routinely processed for electron microscopic examination. After osmium treatment (2%) and contrasting with uranyl acetate (1%), the sections were embedded in Durcupan ACM resin (Fluka). Ultrathin sections (70 nm) were collected on pioloform-coated copper slot grids. Lead citrate contrasting was used only for immunogold/silver labeled sections.

*2.5. Freeze substitution and low temperature embedding in Lowicryl resin*

The procedure was as described earlier (Baude et al., 1993; Nyiri et al., 2001). After washing in PB overnight, the sections were placed into increasing concentration of sucrose solutions (0.5, 1 and 2 M sucrose for 0.5, 1 and 2 h, respectively) for cryoprotection. After slamming onto copper blocks cooled in liquid $N_2$, and following low temperature dehydration and freeze-substitution, the sections were embedded in Lowicryl HM 20 resin (Chemische Werke Lowi, Waldkraiburg, Germany).

*2.6. Postembedding immunocytochemistry on ultrathin sections*

Postembedding immunocytochemistry was with 90 nm thick serial sections of slam-frozen, freeze-substituted, Lowicryl-embedded hippocampi or cerebelli of two adult Thy1α6 mice and one C57BL/6 mouse (Baude et al., 1993; Nyiri et al., 2001). A double-sided reaction was performed, so that antibodies accessed both sides of the sections (Landsend et al., 1997). Sections were picked up on mesh grids coated with coat-quick G-medium (Daido Sangyo Co., Japan) and were treated with a saturated solution on NaOH in 100% ethanol for ~2 s. After washing, the sections were incubated in drops of blocking solution for 1 h, followed by incubation in drops of primary antibodies (5.1 μg/ml) overnight. The blocking solution, which was also used for diluting the primary and secondary antibodies, consisted of 0.05 M Tris–HCl pH 7.4 containing 0.9% NaCl (TBS) and 2% human serum albumin (Sigma). After incubation overnight in primary antibodies, sections were washed in TBS and incubated for 4 h in drops of goat anti-rabbit-IgG coupled to 10 nm gold particles (Britis;.h BioCell Int., UK). Following several washes, sections were contrasted with saturated aqueous uranyl acetate followed by lead citrate.

*2.7. Controls for immunocytochemistry*

No immunofluorescence was detected in the brains of α6−/− mice, confirming the specificity of both primary antibodies. In some incubation the primary antibody was

omitted or replaced with non-immune rabbit IgG of similar protein concentration to those of the affinity purified antibodies. In sections that underwent pre-embedding incubations, only a weak diffuse peroxidase reaction was present and no silver intensified immunogold reaction was detectable, confirming the specificity of the methods. In postembedding immunogold labeling experiments, no labeling was detected at all when the primary antibody was replaced by non-immune rabbit IgG.

### 2.8. Ligand autoradiography

For autoradiography to detect α6βγ2 receptors (Mäkelä et al., 1997), 14-μm horizontal serial sections were cut from five and six frozen brains of wild-type (C57BL/6) and Thy1α6 mice, respectively. Sections were pre-incubated in an ice-water bath for 15 min in 50 mM Tris–HCl (pH 7.4) supplemented with 120 mM NaCl. The final incubation in the pre-incubation buffer was with 10 nM [$^3$H]-labeled ethyl-8-azido-5,6-dihydro-5-methyl-6-oxo-4*H*-imidazo[1,5-*a*][1,4]benzodiazepine-3-carboxylate ([$^3$H]Ro 15-4513; NEN Life Science Products; Boston, MA, USA). For the benzodiazepine-insensitive (DIS) binding, [$^3$H]Ro 15-4513 was allowed to bind to sections in the absence (total binding) and presence of 10 μM diazepam (Orion Pharma, Helsinki, Finland) at 0–4 °C for 60 min. After incubation, sections were washed 3×15 s in the incubation buffer, dipped into distilled water, air-dried under a fan at room temperature, and exposed to Kodak Biomax MR films for eight weeks. The concentration of [$^3$H]Ro 15-4513 (10 nM) was greater than or equal to the dissociation constant for a range of recombinant and native $GABA_A$ receptors; therefore, the autoradiographic images should represent the density rather than affinity of binding sites.

### 2.9. Preparation of membrane extracts, affinity chromatography, immunoprecipitation and Western blot analysis

$GABA_A$ receptors were solubilized from forebrain membranes of Thy1α6 and wild-type mice using a deoxycholate buffer [(0.5% deoxycholate, 0.05% phosphatidylcholine, 10 mM Tris/HCl pH 8.5, 150 mM NaCl, one complete protease inhibitor cocktail tablet per 50 ml buffer (Roche Diagnostics, Mannheim, Germany)] and immunoaffinity chromatography was performed as described (Jechlinger et al., 1998). Briefly, deoxycholate extracts were cycled three times through the affinity column (synthesized as described by Mossier et al., 1994) at a rate of 2 ml/h. To determine the percentage of receptors retained by the column, immunoprecipitations with subunit specific antibodies, followed by [$^3$H]muscimol binding assays were performed with the original extract and the column efflux in parallel (as described in Tretter et al., 2001). Proteins bound to the column were eluted, precipitated and subjected to Western blot analysis as described previously (Jechlinger et al., 1998).

### 2.10. Receptor binding studies

Frozen Thy1α6 forebrain membranes were thawed, homogenized and washed three times with 50 mM Tris/citrate pH 7.1. Extracted receptors were immunoprecipitated and the precipitate was suspended in 0.1% Triton X-100, 50 mM Tris–citrate buffer, pH 7.1. A total of 1 ml of a solution containing 100 μg membrane protein or the resuspended immunoprecipitate was incubated with 2–50 nM of [$^3$H]Ro 15-4513 (21.7 Ci/mmol, Du Pont NEN) in the absence or presence of 100 μM diazepam or 100 μM Ro15-1788, or with 2–50 nM [$^3$H]muscimol (28.5 Ci/mmol Du Pont NEN) in absence or presence of 1 mM GABA, for 90 min at 4 °C. Then the suspensions were filtered through Whatman GF/B filters, the filters were washed with 0.1% Triton X-100, 50 mM Tris–citrate buffer, pH 7.1, and liquid scintillation counted (Tretter et al., 2001).

### 2.11. Antibodies for biochemical studies

The generation of anti-peptide α1(1–9) (Zezula et al., 1991), anti-peptide α6(317–371) (Nusser et al., 1999), anti-peptide β1(350–404) (Jechlinger et al., 1998), anti-peptide β2(351–405), anti-peptide β3(345–408), anti-peptide γ2(319–366) (Tretter et al., 1997), anti-peptide γ3(322–372) (Tögel et al., 1994) or anti-peptide δ (1–44) (Jones et al., 1997) antibodies have been described previously. Anti-peptide α3(338–385), anti-peptide γ1(1–39), and anti-peptide γ3(1–35) antibodies were generated as described by Mossier et al. (1994) and Tögel et al. (1994). The antibodies precipitate exclusively recombinant $GABA_A$ receptors containing the respective subunit, and do not crossreact with other $GABA_A$ receptor subunits (Tretter et al., 2001).

### 2.12. Slice preparation and electrophysiological recordings

Male C57BL/6 wild-type (post-natal day (P)17–32) and Thy1α6 (P18-adult) mice were anaesthetized with either isoflurane or halothane. The brains were rapidly removed and a tissue block adhered to the cutting stage of a Vibrotome (Leica VT1000s, Leica Instruments, Germany), and 350 μm coronal slices of the hippocampus cut in ice-cold artificial cerebrospinal fluid (aCSF) of composition (in mM): NaCl 126; $NaHCO_3$ 26; KCl 2.5; $CaCl_2$ 2; $MgCl_2$ 2; $NaH_2PO_4$ 1.25; glucose 10; and kynurenic acid 3 (Sigma Chemicals, USA and UK), final pH 7.3–7.4 when continuously oxygenated (95% $O_2$, 5% $CO_2$), adjusted with NaOH. Slices (4–6 per hemisphere) were then stored at room temperature in an incubation

chamber containing the above aCSF, but without the kynurenic acid, for at least 1 h. Slices were then transferred to the recording chamber and perfused with warmed (35 ± 1°C, 1–2 ml/min) continuously oxygenated aCSF identical to that used during cutting.

CA1 pyramidal cells were identified using a Zeiss Axioskop (Zeiss, Germany) with a 40× immersion differential interference contrast objective, coupled to an infrared camera system (Hamamatsu, Japan). Whole cell patch clamp recordings were made with an Axopatch 200B or Axopatch 1D amplifier (both Axon Instruments, USA). Patch pipettes (final resistance 3–8 MΩ) contained (in mM): CsCl 135; HEPES 10; $MgCl_2$ 2; $Na_2$-ATP 2; and Na-GTP 0.2, final pH 7.2 adjusted with CsOH. Series resistance (mean at start of experiments, 13.59 ± 0.30MΩ, $n = 82$) and whole-cell capacitance were monitored throughout experiments, and experiments were discontinued if series resistance increased by more than 25–30%. Series resistance was always compensated by 80% using lag values of 7 μs. Experimental data were stored on video or digital audio tape for subsequent analysis.

Kynurenic acid was included in the aCSF during slice preparation to increase slice viability, and during experimental recordings to isolate $GABA_A$ receptor mediated IPSCs. For some experiments, the recorded aCSF also contained tetrodotoxin (TTX, 1 μM), as well as kynurenic acid, to isolate $GABA_A$ receptor-mediated miniature IPSCs (mIPSCs). The benzodiazepine site agonist zolpidem (10 μM) and the α6β2/3-containing $GABA_A$ receptor antagonist furosemide (600 or 60 μM) were bath applied for at least 10 min to determine their effects on mIPSCs. A tonic $GABA_A$ receptor-mediated current component was eliminated by focal application of the $GABA_A$ receptor antagonist 6-imino-3-(4-methoxyphenyl)-1(6*H*)-pyridazinebutanoic acid (SR 95531, 50 μM; Tocris) in the presence of the GABA-uptake blocker 1-[2-([(diphenylmethylene)-imino]oxy)ethyl]-1,2,5,6-tetrahydro-3-pyridinecarboxylic acid (NO-711, 10 μM).

### 2.13. Electrophysiological data analysis

Stored data were digitized at 20 kHz, then low-pass filtered at 2 kHz, using a PCI-MIO 16E-4 data acquisition board (National Instruments, USA), or pClamp software via a DigiData 1200 analogue-to-digital converter (both Axon Instruments). Spontaneous and mIPSCs were detected with amplitude—(threshold typically 5–10 pA) and kinetics-based criteria using in-house, LabView based software (National Instruments) running on a personal computer (Jensen and Mody, 2001). Detected IPSCs were then imported into in-house analysis software, where populations of individual IPSCs in a cell could be averaged, and peak amplitude, frequency and 10–90% rise time measured. The decay of the averaged IPSC in each cell could be fitted with a double exponential, and the weighted decay constant determined using the following formula:

$$\tau_w = \tau_1 A_1 + \tau_2(1-A_1)$$

where, $\tau_w$ is the weighted decay time constant; $\tau_1$ and $\tau_2$, the time constants of the first and second exponential functions; and $A_1$, the proportion of the peak amplitude of the IPSC that is contributed by the first exponential function. Averaged IPSCs were calculated from at least 100 individual IPSCs in each cell, requiring acquisition epochs of at least 30 s, and sometimes longer. The properties of averaged IPSCs and mIPSCs between strains of mice were compared using Student's unpaired *t*-test. The effect of zolpidem and furosemide on averaged mIPSC properties within and between strains was evaluated using Student's paired and unpaired *t*-test, respectively.

We tested for tonic $GABA_A$ receptor mediated currents essentially as described by Nusser and Mody, 2002. An epoch of data was acquired encompassing at least 30 s both before and after focal SR 95531 application. Segments of the baseline current (5 ms) were then detected every 100 ms for the whole acquisition using the detection software, and imported into the analysis software. Since some of the 5 ms segments inevitably lie on spontaneous IPSCs, and are therefore, not representative of the baseline, those segments including values above a threshold for baseline standard deviation (typically 6–8 pA) were regarded as contaminated and removed from the sample population. Three 5-s-periods, one immediately prior to drug onset (BL2) and one each equitemporal before and after drug onset (BL1 and BL3, respectively, see Fig. 8A) were identified, and the mean of the 5 ms baseline segments during each of these three periods was calculated, relative to the mean of the post-drug period. A significant difference, determined using Student's paired *t*-test, between the change in baseline prior to drug onset (i.e. BL1 to BL2, $\Delta_{control}$), and the change in baseline due to drug onset (i.e. BL2 to BL3, $\Delta_{SR95531}$), across the whole cell population for each mouse strain identifies the presence of a tonic current. The apparent amplitude of the tonic current ($I$) was calculated by subtracting $\Delta_{control}$ from $\Delta_{SR95531}$. Difference in the amplitude of $\Delta_{SR95531}$, and the apparent amplitude of the tonic current, between mouse strains was determined using Student's unpaired *t*-test.

Analysis of the variance of the baseline standard deviation prior to and after SR 95531 onset for each cell enabled us to determine the single channel current of the receptors mediating the tonic current, using the following formula:

$$i = (\sigma^2_{BL1} - \sigma^2_{BL3}) / \Delta_{SR95531} - \Delta_{control})$$

where, $i$ is the single channel current, $\sigma^2_{BL1}$ and $\sigma^2_{BL3}$ are the variances of the baseline standard deviation of BL1

and BL3; and $\Delta_{control}$ and $\Delta_{SR95531}$ are the changes in baseline current prior to and after SR 95531 application, as outlined before. Following this, the single channel conductance ($g$) of the receptors mediating the tonic current can be determined using the following equation:

$$g = i/(V_m - E_{Cl})$$

where $i$ is the single channel current, $V_m$ is the holding potential of the cell (approximately −60 mV) and $E_{Cl}$ the reversal potential for $Cl^-$, in this instance approximately 0 mV. Single channel conductance was calculated only for cells that had apparent tonic current amplitude greater than 5 pA. Difference in the single channel conductance between mouse strains was tested using Student's unpaired $t$-test. Division of the tonic current amplitude ($I$) by the single channel current ($i$) gives the mean number of open channels underlying the tonic current.

In all cases data are expressed as mean±SEM. The significance for comparison using both Student's paired and unpaired $t$-test was set at $p < 0.05$. Data were recorded from 43 and 39 CA1 pyramidal cells of C57BL/6 mice, and Thy1α6 mice, respectively. All experiments were performed at a holding potential of −60 mV (−60.29 ± 0.17mV, $n = 82$).

### 2.14. Solutions and drugs for electrophysiology

Drugs and their sources were: Kynurenic acid, NO711 and furosemide (Sigma Chemicals, UK); TTX (Sigma and Tocris, Bristol, UK); SR 95531 and zolpidem (Tocris). Both zolpidem and furosemide were dissolved first in dimethyl sulfoxide (DMSO, Sigma) before addition to the aCSF. For zolpidem, the final concentration of DMSO in the aCSF was 1:10000, whereas for furosemide it was 1:2000 at 600 μM concentration, and 1:20000 for 60 μM.

## 3. Results

### 3.1. Generation of Thy1α6 transgenic mice and expression of the Thy1α6 gene

We generated mice in which the $GABA_A$ receptor α6 subunit is ectopically expressed in the brain by using the Thy-1.2 transgene cassette (Caroni, 1997; Fig. 1 and Methods). Thy-1 is a universally expressed neuronal gene; depending on the random integration position of the corresponding transgene in the mouse genome, different but inheritably stable patterns of transgene expression are produced (Caroni, 1997). Fig. 1A shows the expression of the Thy1α6 transgene as seen by mRNA in situ hybridization to adult brain sections. Transgene expression was specifically detectable with an oligonucleotide that hybridizes to the introduced Flag nucleotide sequence marking Thy1α6 transcripts. Strong transgene expression was found in many brain regions; for example, deep cerebellar nuclei, deep layers of neocortex (layer V stronger than layer VI), layer II of neocortex in the somatosensory area, hippocampal pyramidal cells and dentate granule cells, cells throughout the colliculi, cells in the septum, and olfactory bulb mitral cells (Fig. 1A and B). Unlike the native α6 gene (Fig. 1C), the Thy1α6 transgene was not expressed in cerebellar granule cells. Western blots with an α6 subunit-selective antibody showed a 57 kDa band in Thy1α6 but not C57BL/6 wild-type forebrain membranes (Tretter and Sieghart, data not shown), thus, confirming that the Thy1α6 mRNA was translated to a subunit of the expected size.

### 3.2. Extra-cerebellar expression of the α6 subunit protein in Thy1α6 mice

Consistent with the in situ hybridization results, immunofluorescence labeling revealed a widespread but selective expression of the α6 subunit from the rostral isocortex through to the caudal brain stem in Thy1α6 but not in C57BL/6 (wild-type) mice (Fig. 2) (note: in both wild-type and transgenic brains the cerebellar granule cell layer was strongly α6-immunopositive (not shown) resulting from the native α6 subunit gene expression e.g. see Fig. 1C for native α6 mRNA). In any given Thy1α6 brain area only some of the cells were α6-immunopositive (Fig. 2). In general, but not always, large cell types showed strong expression. In the isocortex, most of the largest pyramidal cells were α6-immunopositive in layer V, particularly in frontal and parietal areas (Fig. 2). In the hippocampal formation, the strongest expression was in the subiculum, followed by CA1 pyramidal cells, some of the CA3 pyramidal cells and most dentate granule cells (Fig. 2A). The CA2 pyramidal cells were immunonegative. Particularly strong α6 subunit expression was present in the globus pallidus and zona reticulata of the substantia nigra, the nucleus ruber, the large cells in the intermediate gray layer of the superior colliculus, some cells of the pontine nuclei, the vestibular nuclei, the deep cerebellar nuclei, the gigantocellular reticular formation, the trigeminal nucleus and the lateral reticular nucleus. A notable immunonegative large-sized cell population was the Purkinje cells.

In all areas α6 immunoreactivity was present in the cell body and extended along the dendrites to varying degrees, in some cases clearly delineating the plasma membrane. For example, the entire somato-dendritic surface of layer V pyramidal cells was immunopositive (Fig. 2C and D) and also outlined all the dendritic spines (Fig. 2E). Similarly, in the subiculum and CA1 hippocampal area, the entire somato-dendritic domain of the pyramidal cells was strongly and uniformly α6 subunit-immunopositive. This α6 subunit distribution did not

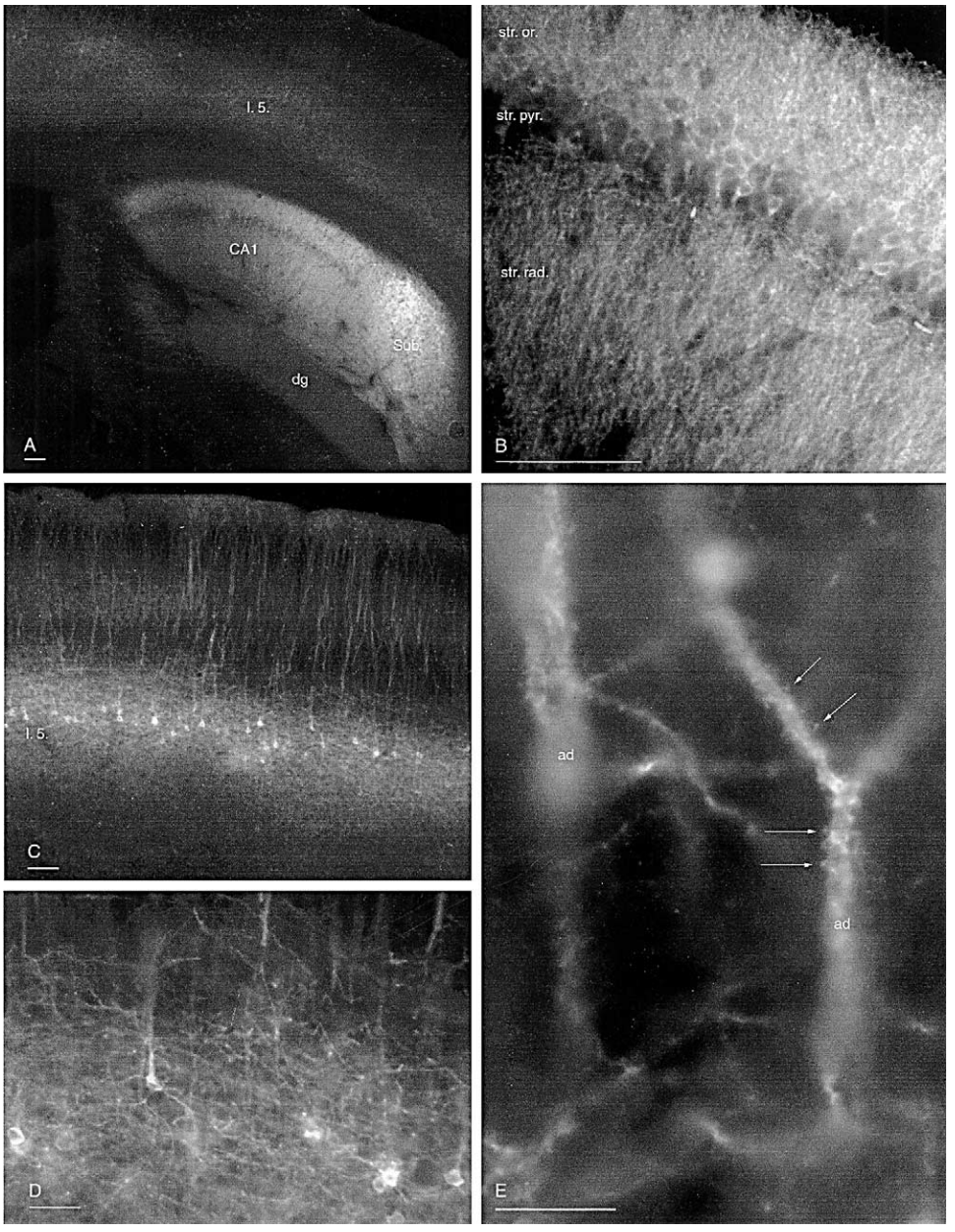


Fig. 2. Expression of the $GABA_A$ receptor α6 subunit in forebrain neurones of the Thy1α6 mouse. Immunofluorescence detection with antibody to the N-terminal part of the subunit. A. Parasagittal section of the brain showing strong expression of the α6 subunit in the subiculum (Sub) and the CA1 hippocampal areas, and weaker immunoreactivity in layer 5 of the isocortex (l.5.) and the dentate gyrus (dg). B. Higher magnification view of the CA1 area demonstrating the subunit throughout the somatic and dendritic membranes of pyramidal cells with clearly labeled cell bodies is stratum pyramidale (str. pyr). C–E. Strong expression of the α6 subunit in a subpopulation of large layer 5 (l.5.) pyramidal cells in the frontal cortex. The subunit is present throughout the somato-dendritic surface of the cells, including the apical dendrites (ad) and the dendritic spines (e.g. arrows). Scales: A–D, 100 μm; E, 20 μm.

seem to follow the known density of GABAergic terminals innervating these cells. The surface α6 subunit immunolabeling also seemed uniform in other strongly α6 subunit-immunopositive cell types. In addition to the surface labeling, immunoreactivity was present intracellularly (excluding the nucleus). This intracellular α6 subunit pool may have corresponded to protein in the process of synthesis in the endoplasmic reticulum or to partially assembled receptors.

### *3.3. Assembly of Thy1-expressed α6 subunit with other $GABA_A$ receptor subunits: widespread formation of α6βγ2 receptors and absence of α6βδ receptors*

The Thy1α6 brains were analyzed by ligand binding and protein biochemistry to confirm and probe how the forebrain-expressed α6 subunit assembles with native $GABA_A$ receptor subunits. α6βγ2 receptors can bind the benzodiazepine partial inverse agonist Ro 15-4513 but

cannot bind benzodiazepine full agonists such as diazepam (Lüddens et al., 1990; Barnard et al., 1998; Hevers and Lüddens, 1998). This property can be used to cleanly assay for α6-containing receptors which also contain a γ2 subunit (Mäkelä et al., 1997). Fig. 3 shows autoradiography of the α6 subunit-specific binding component (DIS binding of [$^3$H]Ro 15-4513) in Thy1α6 and wild-type brains. The characteristic signature of α6βγ2 receptors, confined to the cerebellar granule cell layer of non-transgenic mice, was additionally present in brain regions of Thy1α6 mice in a pattern (Fig. 3) in good agreement with that obtained by in situ hybridization (Fig. 1) and α6-immunocytochemistry (Fig. 2). DIS binding highlighted particularly the CA1 area of hippocampus and the inner layers of the neocortex (Fig. 3), suggesting the assembly of the transgenic α6 subunit into α6βγ2 receptors in these brain regions.

Consistent with the autoradiographic results, Scatchard analysis ($n$ = 4) with [$^3$H]Ro 15-4513 on membranes prepared from wild-type and Thy1α6 mice forebrains gave a 28% increase of Ro15-4513 binding in the Thy1α6 over wild-type (not shown); most of this increased binding (approximately 80%) was DIS binding (data not shown) suggesting that many of the forebrain α6 subunits assembled into α6βγ2 receptors. To examine the receptor subunit composition of the α6-containing receptors in Thy1α6 brains in more detail, forebrain receptors were extracted and chromatographed on a α6-immunoaffinity column. The column was washed and the receptors were then eluted, precipitated, electrophoresed and Western blotted. In addition to α6 subunits, α1, α3, β1, β2, β3 and γ2 subunits were retained by the column, and could be detected in the column eluate (Fig. 4), consistent with the formation of α6βγ2, α1α6βγ2 and α3α6βγ2 receptors. No α4, α5 or δ subunits could be identified. Detection sensitivity, however, depends not only on the total subunit amount, but also on the efficiency of the antibodies for labeling the subunits and so the signals do not reflect the actual amounts of receptors containing these subunits. Absence of labeling does not necessary mean that these subunits are not there. It is possible that subunits only present in small amounts are below the detection limit of the antibody. To confirm these column purification data and to get a quantitative estimate, we immunoprecipitated receptors using α6-, γ2-, or δ-specific antibodies and then did muscimol binding assays, both before and after the α6 column; comparable amounts (fmoles/mg protein) of α6 and γ2 subunit-containing receptors were eliminated by the column, but the amount of δ subunit containing receptors present in the original extract was barely reduced, indicating that if α6βδ receptors do form in Thy1α6 forebrains, they make a minor contribution (data not shown). This again indicates that most α6 receptors in Thy1α6 forebrain contained γ2 subunits.

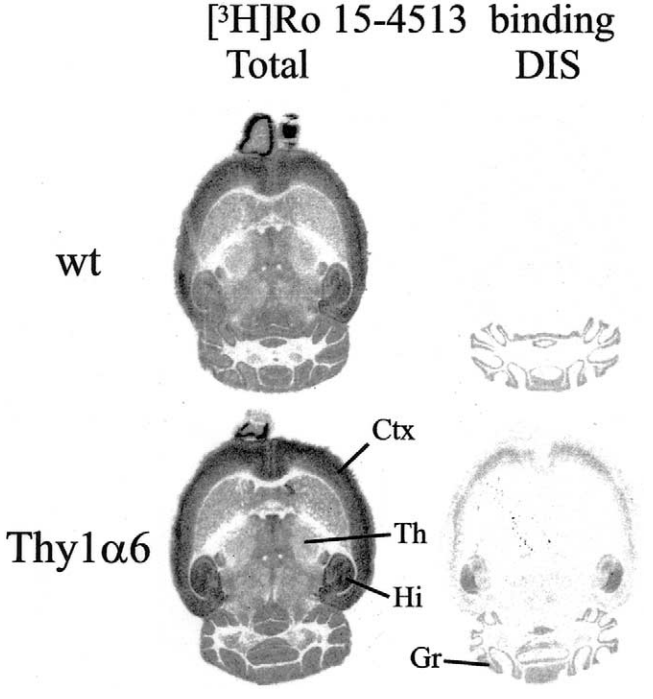


Fig. 3. Autoradiographic images of [$^3$H]Ro 15-4513 binding to wild-type and Thy-1 α6 mouse brain sections. [$^3$H]Ro 15-4513 binding was studied in the absence and presence of 10 μM diazepam to reveal the α6 subunit-selective DIS binding component. Ctx: cortex; Gr: cerebellar granule cell layer; Hi: hippocampus; Th: thalamus. Images for wild-type and Thy-1 α6 mouse brains were processed from the same films with identical scaling for brightness and contrast.

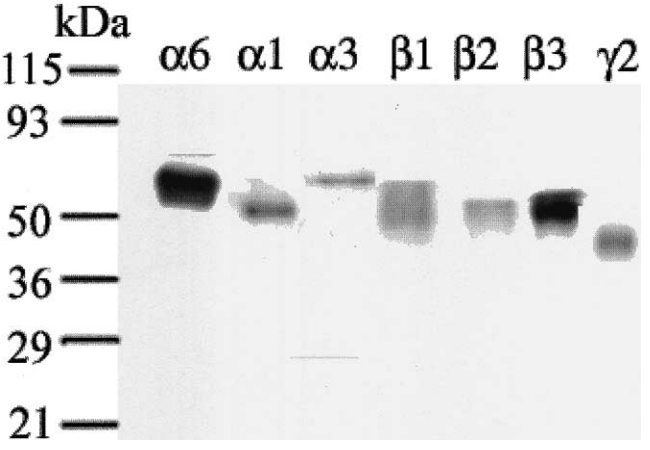


Fig. 4. Western blots indicating $GABA_A$ receptor subunits co-purifying with Thy1α6 subunits on an α6(317–371)-immunoaffinity column. Thy1α6 forebrain extracts were chromatographed on an α6(317–371) immunoaffinity column. The column was washed, eluates of the column were precipitated and the precipitates were subjected to SDS-Page and Western blot analysis using the following digoxigenated antibodies: α1(1–9), α6(317–371), α3(338–385), β1(350–404), β2(351–405), β3(345–408) and γ2(319–366). The antibodies used selectively recognized their respective subunit and did not display any cross-reactivity with other $GABA_A$ receptor subunits. Intensity of labeling does not reflect the amounts of subunit present, because the individual antibodies exhibit different labeling efficiencies. The experiment was performed three times with comparable results.

### *3.4. Subcellular localization of α6 subunit immunoreactivity in forebrain neurons*

To investigate the subcellular distribution of α6 subunits in the Thy1α6 forebrain, two strongly α6-immunopositive cell types, the layer V isocortical and the CA1 hippocampal pyramidal cells were chosen on the basis of their well characterized synaptic responses and known GABAergic innervations (Somogyi et al., 1998). In the hippocampal CA1 area of Thy1α6 mice, pre-embedding immunoperoxidase labeling using the α6(317–371) antibodies showed a homogeneous intracellular labeling, in accordance with the α6 subunit epitope being cytoplasmic. The peroxidase product covered all organelles and synaptic specializations, filling also the dendritic spines (Fig. 5A). The pre-embedding immunogold labeling showed that most of the immunoreactivity associated with the extrasynaptic plasma membrane of dendrites (Fig. 5A–C), including the extrasynaptic membrane of dendritic spines (Fig. 5A–C). Postembedding immunogold reactions in addition showed clear labeling of type II synaptic junctions on pyramidal cell somata (Fig. 5D) and dendrites (Fig. 5E). Synaptic labeling was rare and few particles were found in labeled synapses.

In layers II–V of the isocortex of Thy1α6 mice, α6-immunopositive dendrites were easily identified both in immunoperoxidase (not shown), and pre-embedding immunogold labeling (Fig. 6). Immunogold labeling was mostly along the plasma membranes and strongest on the extrasynaptic membrane of dendrites (Fig. 6A and C) and dendritic spines (Fig. 6B). In addition, immunolabeling occured occasionally at the postsynaptic mem-

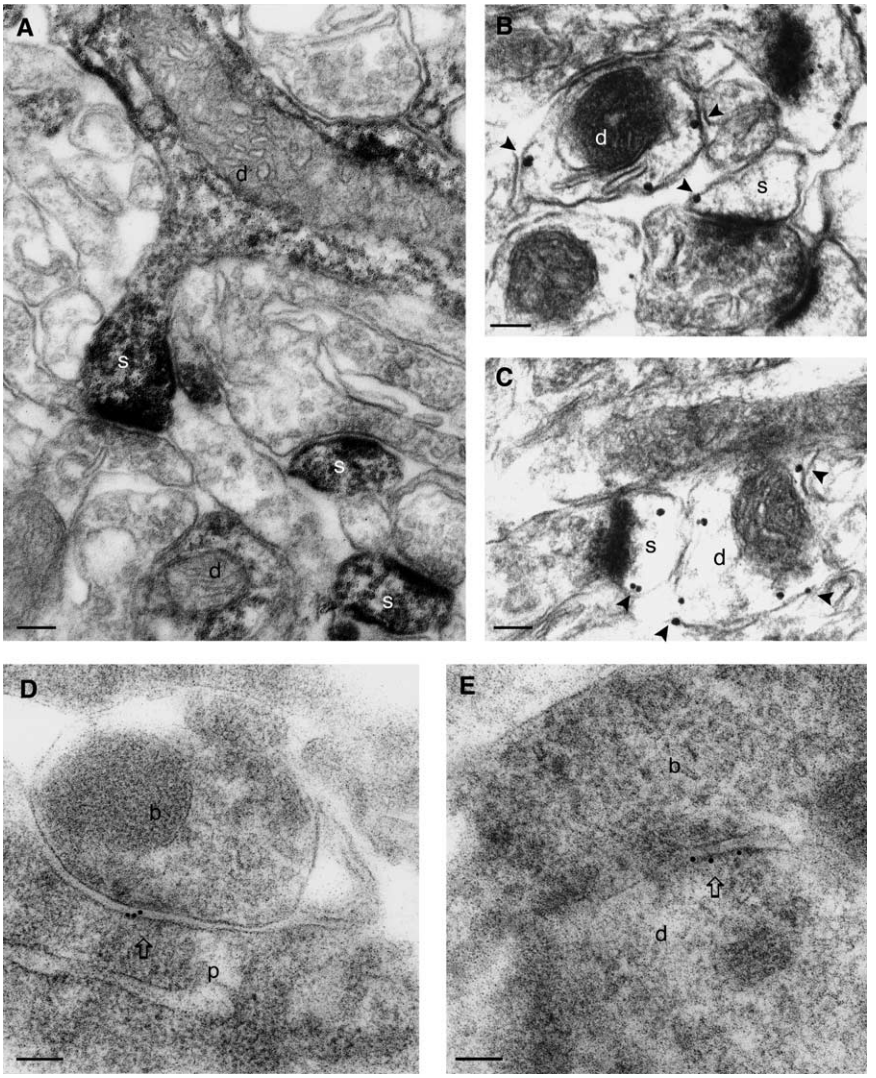


Fig. 5. Subcellular distribution of immunoreactivity for the $GABA_A$ receptor α6 subunit in the hippocampal CA1 area of Thy1α6 mice. A. Electron micrograph showing immunoperoxidase reaction. Peroxidase reaction product for the α6 subunit is present in dendritic spines (s) as well as in dendrites (d) of pyramidal cells. B–C. Pre-embedding silver-intensified immunogold reaction revealed labeling (e.g. arrowheads) for the α6 subunit on extrasynaptic membranes of dendrites and spines. D–E. Postembedding immunogold reaction showed immunolabeling for the α6 subunit (10 nm gold particles) in type II synaptic junctions (open arrows) on the soma of a pyramidal cell (p) and on a dendrite (d) formed by presumed GABAergic boutons (b). Scale: bars 0.1 μm (A–E).

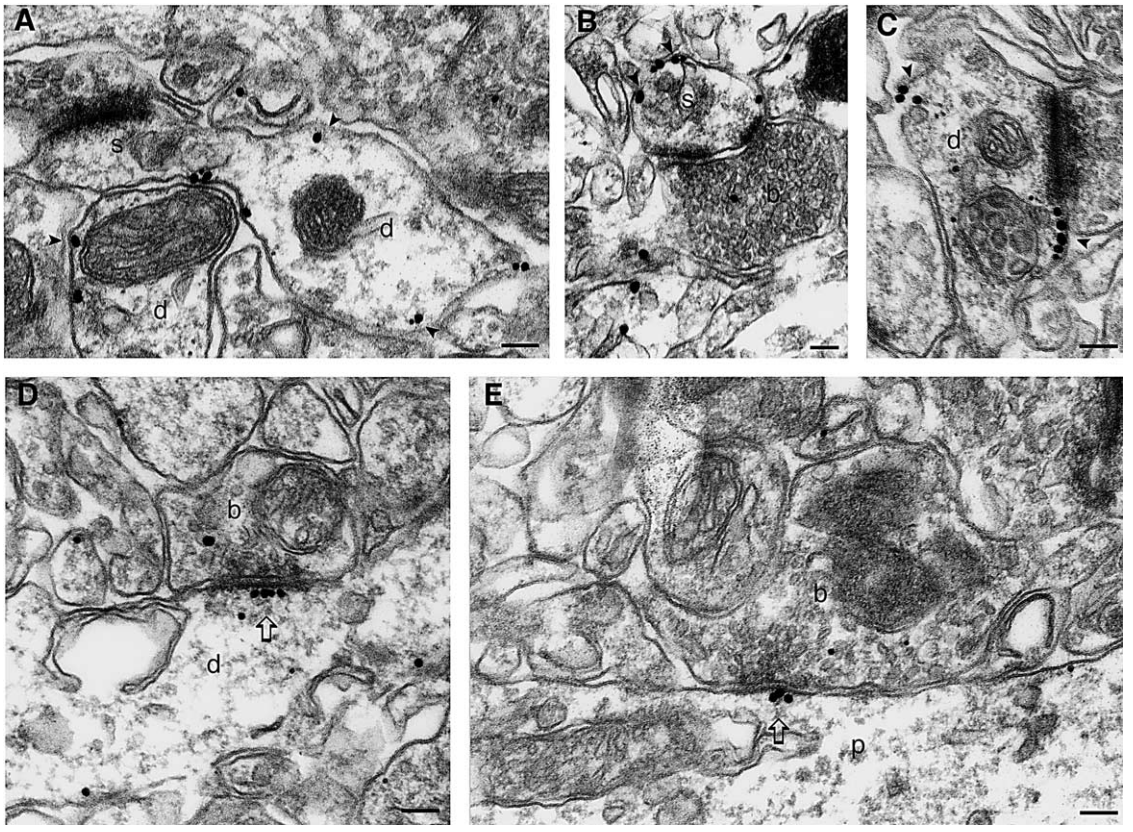


Fig. 6. Subcellular distribution of immunoreactivity for the $GABA_A$ receptor α6 subunit in layer V of the isocortex as revealed by a pre-embedding, silver-intensified immunogold reaction. A. Electron micrograph showing pyramidal cell dendrites (d) and a spine (s). Immunoparticles (e.g., arrowheads) are present along the extrasynaptic membranes. B, C. The extrasynaptic membranes of a spine and a dendrite are strongly immunolabeled for the α6 subunit (arrowheads). D–E. A dendrite and the soma of a pyramidal cell (p) receive type II synapses (open arrows) from presumed GABAergic boutons (b). The postsynaptic membrane specializations (open arrows) are immunolabeled for the α6 subunit. Scale: bars 0.1 μm (A–E).

brane specialization of type II (GABAergic) synapses on dendrites (Fig. 6D), as well as on pyramidal cell somata (Fig. 6E) in layer V. Type I synapses were immunonegative.

### *3.5. Spontaneous, action potential-dependent and -independent IPSCs in Thy1α6 CA1 pyramidal cells*

To examine if the non-synaptic localization of the α6βγ2 receptors in hippocampal CA1 pyramidal cells had functional consequences we looked at the electrophysiological properties of synaptic and extrasynaptic $GABA_A$ receptor-mediated responses in hippocampal slices prepared from wild-type (C57BL/6) and Thy1α6 brains.

We first described the basic parameters of fast inhibitory synaptic transmission onto CA1 pyramidal cells. Spontaneous IPSCs recorded in CA1 pyramidal cells of C57BL/6 mice, in the presence of 3 mM kynurenic acid to block ionotropic glutamate receptors (Fig. 7A), had a mean frequency of 19.75 ± 2.38Hz (range 8.68–36.61 Hz, $n = 14$), compared with a mean of 12.61 ± 1.33Hz (4.84–21.11 Hz, $n = 15$; $p < 0.05$) in CA1 pyramids of Thy1α6 mice (Fig. 7C). The peak amplitude of the averaged IPSC for C57BL/6 mice was −46.32 ± 2.27pA ($n = 14$), and this was not significantly different to that observed in Thy1α6 mice (−44.62 ± 2.80pA, $n = 15$; $p > 0.5$) (Fig. 7B and C). Similarly, the weighted decay time constant ($\tau_w$) of the averaged IPSC was not significantly different between the C57BL/6 and Thy1α6 mice (C57BL/6 = 4.12 ± 0.27ms, $n = 14$; Thy1α6 = 4.72 ± 0.34ms, $n = 15$; $p > 0.1$) (Fig. 7B and C), nor is the 10–90% rise time different (C57BL/6 = 0.34 ± 0.02, $n = 14$; Thy1α6 = 0.31 ± 0.02, $n = 15$; $p > 0.1$). The spontaneous IPSCs recorded under such conditions in both wild-type C57BL/6 and Thy1α6 mice disappeared after focal application of the $GABA_A$ receptor specific antagonist SR95531 (50 μM), and therefore, solely depended on activation of $GABA_A$ receptors (C57BL/6, $n = 14$; Thy1α6, $n = 15$) (data not shown).

### *3.6. Increased tonic, $GABA_A$ receptor-mediated current in Thy1α6 CA1 pyramidal cells*

Because of the marked extrasynaptic location of $GABA_A$ receptors containing the α6 subunit on CA1 pyramidal cells we tested the tonic inhibitory current in

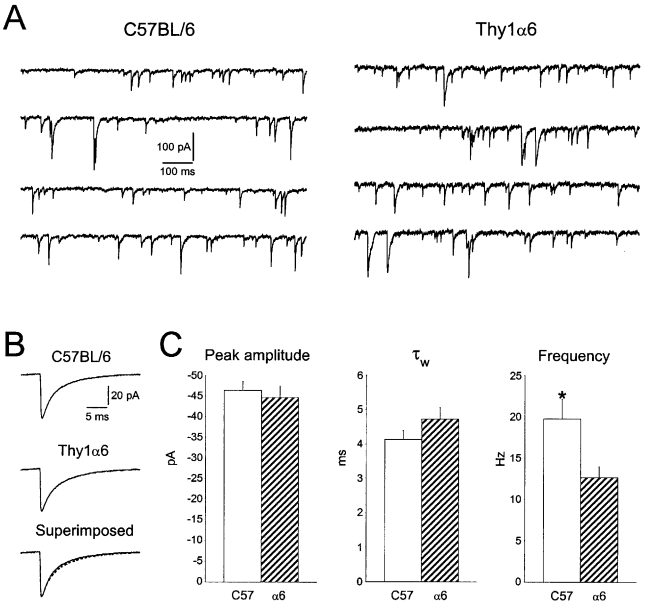


Fig. 7. Comparison of spontaneous $GABA_A$ receptor mediated IPSCs in CA1 pyramidal cells of C57BL/6 and Thy1α6 mice. A. Series of 1 s epochs of spontaneous IPSCs recorded from a CA1 pyramidal cell of a C57BL/6 mouse (left) and a Thy1α6 mouse (right), respectively, in the presence of kynurenic acid (3 mM). B. Comparison of the waveform of the averaged IPSC for the cells depicted in A and superimposition of the normalized averaged IPSCs (solid line, C57BL/6; dashed line, Thy1α6). C57BL/6, peakamplitude = −48.63pA, $\tau_w$ = 4.12ms, 10–90% risetime = 0.29ms ($n$ = 310 individual events); Thy1α6, peakamplitude = −46.59pA, $\tau_w$ = 4.61ms, 10–90% risetime = 0.21ms ($n$ = 481 individual events). C. Comparison of peak amplitude, $\tau_w$ and frequency between C57BL/6 ($n$ = 14 cells) and Thy1α6 ($n$ = 15 cells) mice. * = $p < 0.05$ (Student's unpaired $t$-test).

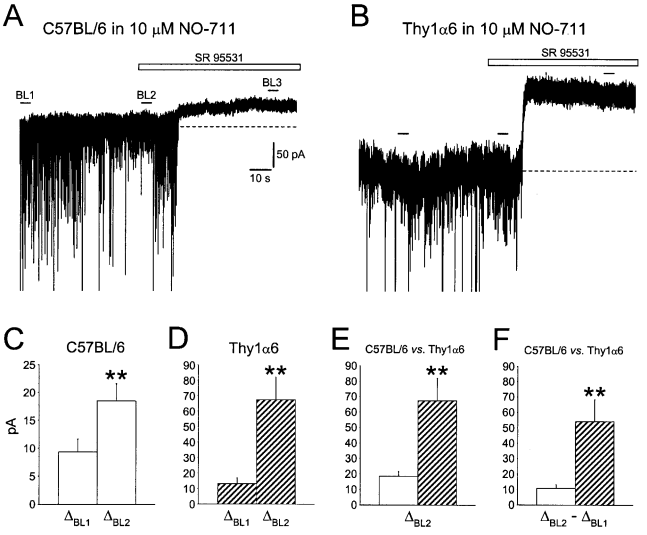


Fig. 8. CA1 hippocampal pyramidal cells of Thy1α6 mice exhibit a larger $GABA_A$ receptor mediated tonic current than those of C57BL/6 mice. A and B. Determination of the presence of a tonic current following focal application of the $GABA_A$ receptor antagonist SR 95531 (50 μM, white bar), in the presence of kynurenic acid (3 mM) and the GABA uptake blocker NO-711 (10 μM). Notice the positive shift in baseline current following the onset of the drug, identified by cessation of the inward spontaneous events (dotted line is the approximate continuation of the initial baseline current). Horizontal black bars (BL1, BL2 and BL3) indicate the five second epochs used to calculate the presence of the tonic current (see Methods for details). C and D. Comparison of the baseline currents prior ($\Delta_{control}$, marked $\Delta_{BL1}$ in figure) and subsequent to ($\Delta_{SR95531}$, marked $\Delta_{BL2}$ in figure) drug onset in C57BL/6 ($n$ = 12cells) and Thy1α6 mice ($n$ = 9cells), respectively. E. Comparison of the shift in baseline current caused by SR 95531 ($\Delta_{SR95531}$, marked $\Delta_{BL2}$ in figure) between C57BL/6 and Thy1α6 mice. F. Comparison of the calculated tonic current ($\Delta_{SR95531} - \Delta_{control}$, marked $\Delta_{BL2} - \Delta_{BL1}$ in figure) between C57BL/6 and Thy1α6 mice. C–F, ** = $p < 0.005$ (Student's paired and unpaired $t$-test). Calibration bars in A also apply to B.

these cells. Tonic current was assayed as follows: the antagonist SR95531 was applied, and any difference between baseline current pre- and post-drug application was assumed to be the tonic current. However, the baseline current prior to SR95531 application was not stable, and drifted during recording. Thus, we aimed to measure significant differences between the drift of the baseline current prior to SR95531 application ($\Delta_{control}$), and the shift in the baseline current caused by the action of SR95531 ($\Delta_{SR95531}$) (Nusser and Mody, 2002). In the presence of 3 mM kynurenic acid, SR95531 (50 μM) blocked $GABA_A$ receptor mediated IPSCs, but did not reveal a tonic $GABA_A$ receptor mediated current in either wild-type C57BL/6 ($n$ = 14) or Thy1α6 mice ($n$ = 15) (data not shown). Because this lack of effect may have been due to low ambient GABA levels in the continuously perfused slice, the experiment was repeated with the GABA uptake blocker (GAT-1 antagonist) NO-711 (10 μM) in the aCSF to increase GABA concentration in the extracellular space (Borden et al., 1994; Frahm et al., 2001; Nusser and Mody, 2002). Focal application of SR 95531 (50 μM) in the presence of kynurenic acid and NO-711 not only abolished spontaneous IPSCs in cells from C57BL/6 and Thy1α6 mice, but also revealed a tonic $GABA_A$ receptor mediated current, evident as a positive shift in the baseline current of the cell (Fig. 8A and B). Comparing the shift in baseline current caused by the onset of SR 95531 ($\Delta_{SR95531}$) to a period of quiescent baseline prior to SR 95531 onset ($\Delta_{control}$) revealed a tonic current in both C57BL/6 ($n$ = 12; $p < 0.01$) and Thy1α6 mice ($n$ = 9; $p < 0.01$) (Fig. 8C and D, respectively). Comparison of $\Delta_{SR95531}$ caused by SR 95531 application between C57BL/6 and Thy1α6 mice revealed a significantly larger tonic $GABA_A$ receptor mediated current in Thy1α6 mice ($n$ = 12 vs. 9, respectively; $p < 0.001$) (Fig. 8E). Subtracting $\Delta_{control}$ from $\Delta_{SR95531}$ gave a measure of the size of the tonic current. This was approximately five-fold larger in the Thy1α6 (54.10 ± 14.16pA, $n$ = 9) compared with the C57BL/6 wild-type mice (10.72 ± 2.32pA, $n$ = 12; $p < 0.01$) (Fig. 8F). Similarly, the calculated conductance of the tonic current was five-fold larger in the Thy1α6 mice (Thy1α6 = 902.53 ± 238.45pS, $n$ = 9; C57BL/6 = 176.08 ± 37.55pS, $n$ = 12; $p < 0.01$). Importantly, comparison of the change in baseline cur-

rent prior to SR 95531 onset (i.e. $\Delta_{control}$) between C57BL/6 (9.33 ± 2.31pA) and Thy1α6 (13.22 ± 3.72pA) mice gave no significant difference ( $n = 12$ vs. 9; $p > 0.1$). Therefore, the presence of a larger tonic $GABA_A$ receptor-mediated current could not be explained by different initial experimental conditions between the C57BL/6 and Thy1α6 mice.

The extrasynaptic locus of the α6 subunit containing receptors was supported by comparison of the baseline standard deviation prior and subsequent to SR 95531 onset, which revealed a significant $GABA_A$ receptor contribution to the baseline noise in both C57BL/6 ( pre = 6.30 ± 0.29pA, post = 5.40 ± 0.24pA, $n = 12$; $p < 0.001$) and Thy1α6 mice (pre = 7.11 ± 0.30pA, post = 5.20 ± 0.29pA, $n = 9$; $p < 0.001$). Thus, in both C57BL/6 and Thy1α6 mice, extrasynaptic receptors contributed to baseline noise. However, calculation of the single channel conductance of the extrasynaptic $GABA_A$ receptors underlying the tonic current showed no difference between mouse strains (C57BL/6 = 14.27 ± 3.26pS, $n = 8$; Thy1α6 = 12.63 ± 5.37pS, $n = 9$; $p > 0.5$). Therefore, the larger tonic current in the Thy1α6 mice probably arose from more extrasynaptic receptors compared with those in the C57BL/6 mice. Calculation of the mean number of open channels generating the tonic current in C57BL/6 (approximately 12) and Thy1α6 mice (approximately 71) indicated this was the case, and was a further indication that the α6 subunit was incorporated into functional extrasynaptic receptors in the Thy1α6 mice (note: receptors in the synaptic junction may also contribute to baseline noise if activated by GABA released at distant synapses and diffusing into the synaptic cleft from the non-synaptic extracellular space).

Spontaneous IPSCs recorded in the presence of 10 μM NO-711 showed little difference between C57BL/6 and Thy1α6 mice, except that as under control conditions the frequency of IPSCs tended to be lower in Thy1α6 mice (C57BL/6 = 9.62 ± 1.41Hz, $n = 12$; Thy1α6 = 5.71 ± 0.78Hz, $n = 7$; $p = 0.06$). No significant difference was found in the peak amplitude (C57BL/6 = −44.72 ± 2.71pA, $n = 12$; Thy1α6 = −38.31 ± 2.92pA, $n = 7$; $p > 0.1$), $\tau_w$ (C57BL/6 = 5.67 ± 0.29ms, $n = 12$; Thy1α6 = 4.95 ± 0.49ms, $n = 7$; $p > 0.1$) or the 10–90% rise time (C57BL/6 = 0.37 ± 0.02ms, $n = 12$; Thy1α6 = 0.39 ± 0.04ms, $n = 7$; $p > 0.5$) of the averaged IPSCs.

### 3.7. mIPSCs in Thy1α6 CA1 pyramidal cells

Addition of the voltage-activated sodium channel blocker TTX (1 μM) to the aCSF, in the continuing presence of kynurenic acid (3 mM) to block ionotropic glutamate receptors, isolated action potential-independent mIPSCs. These mIPSCs arose by spontaneous quantal release of GABA from pre-synaptic terminals (Fig. 9A). The mIPSC frequency was not significantly different between C57BL/6 (16.89 ± 2.81Hz, $n = 17$) and Thy1α6 (13.39 ± 1.87Hz, $n = 15$; $p > 0.1$) mice. However, the peak amplitude of the averaged mIPSC was significantly larger in C57BL/6 wild-type compared with Thy1α6 mice (−42.04 ± 2.73vs. −29.74 ± 2.89pA, $n = 17$ and 15, respectively $p < 0.01$) (Fig. 9B), but $\tau_w$ (4.43 ± 0.16ms vs. 4.87 ± 0.27ms, $n = 17$ and 15; $p > 0.1$) (Fig. 9B) and the 10–90% rise time (0.32 ± 0.01ms vs. 0.33 ± 0.02ms, $n = 17$ and 15; $p > 0.5$) were not.

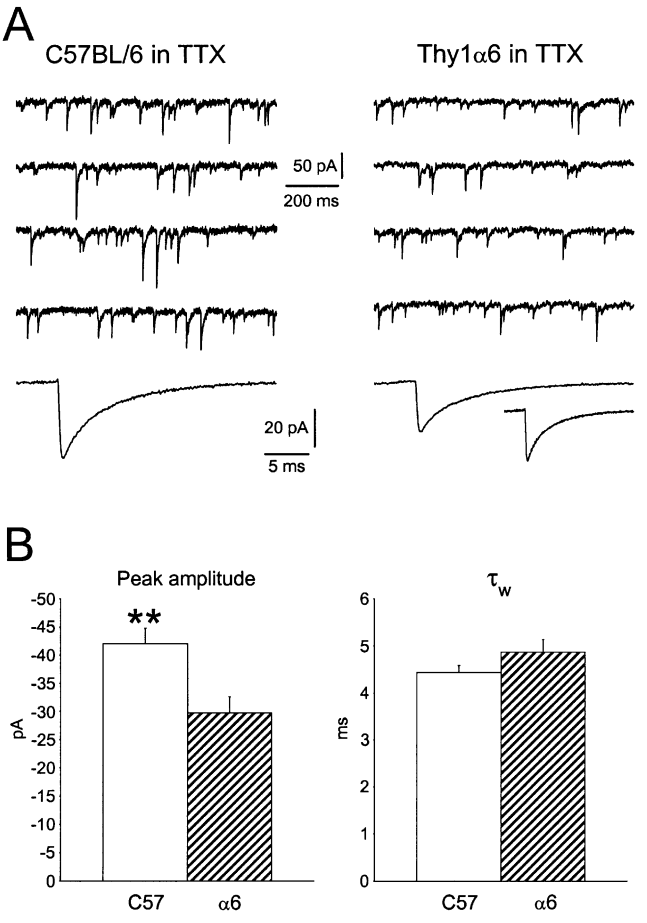


Fig. 9. Comparison of $GABA_A$ receptor mediated mIPSCs in CA1 pyramidal cells of C57BL/6 and Thy1α6 mice. A. Series of mIPSCs, and the waveform of the averaged mIPSC, recorded from a CA1 pyramidal cell of a C57BL/6 mouse (left) and a Thy1α6 mouse (right), in the presence of kynurenic acid (3 mM) and TTX (1 μM). Properties of the averaged mIPSCs: C57BL/6, peakamplitude = −41.01pA, $\tau_w$ = 4.92ms 10–90% risetime = 0.28ms ($n = 275$ individual events); Thy1α6, peakamplitude = −26.65pA, $\tau_w$ = 5.11ms, 10–90% risetime = 0.29ms ($n = 279$ individual events). Inset depicts superimposed traces of the normalized averaged mIPSCs (C57BL/6, solid line; Thy1α6, dashed line). B. Comparison of peak amplitude and $\tau_w$ between C57BL/6 ($n = 17$cells) and Thy1α6 ($n = 15$cells). ** = $p < 0.005$ (Student's unpaired $t$-test).

### 3.8. Testing for α6-containing $GABA_A$ receptors in Thy1α6 CA1 pyramidal cell synapses: effect of furosemide and zolpidem on synaptic responses

The electron microscopy data showed that rare α6-subunit positive synapses existed on CA1 pyramidal

cells (Fig. 5). To evaluate the overall significance of these infrequent α6 subunit-positive synapses, we used a global measure, synaptic response. If significant numbers of α6-subunit containing synapses were present on any given CA1 pyramidal cell, we would have expected the pharmacology of the synaptic response to change. Most wild-type CA1 pyramidal cell mIPSCs we recorded probably derived from synapses contacting the soma; many of these synapses would have contained α1 $GABA_A$ receptor subunits, probably in an α1β2/3γ2 configuration (Klausberger et al., 2002; Nusser et al., 1996a; Somogyi et al., 1996). But in the Thy1α6 mice the receptor composition in some of these same CA1 pyramidal synapses might have been α1α6βγ2 and/or α1βγ2 together with α6βγ2. On cerebellar granule cells, α6-containing receptors in α6βγ2 and α1α6βγ2 configurations are synaptic and contribute to synaptic currents (Nusser et al., 1996a,b; Mellor et al., 2000); however, IPSCs on some cerebellar granule cells have reduced responses to benzodiazepine agonists because of a dominant influence of the synaptic α6 subunit over the α1 subunit with respect to benzodiazepine pharmacology (Sigel and Baur, 2000; Hevers and Lüddens, 2002); furthermore, granule cells with no α6 subunits are more benzodiazepine-sensitive (Jones et al., 1997; Korpi et al., 1999). By analogy, these factors suggest that in Thy1α6 CA1 pyramidal cells any significant numbers of synaptically located α6 subunits will decrease the benzodiazepine response of $GABA_A$ receptor subtypes.

Bath application of 10 μM zolpidem (an α1β2-selective benzodiazepine agonist—Barnard et al., 1998; Hevers and Lüddens, 1998) does not significantly change the mIPSC frequency in either C57BL/6 (pre-zolpidem = 20.91 ± 466 Hz, post-zolpidem = 23.46 ± 6.04 Hz $n = 9$; $p > 0.1$) or Thy1α6 mice (pre = 13.85 ± 3.28Hz, post = 15.83 ± 3.55Hz, $n = 7$; $p > 0.1$). In addition, there is no significant increase in the peak amplitude for either C57BL/6 (pre = −45.06 ± 3.63pA, post = −48.43 ± 3.51pA, $n = 9$; $p > 0.1$) or Thy1α6 mice (pre = −34.14 ± 5.61pA, post = −40.58 ± 7.52pA, $n = 7$; $p > 0.1$). In contrast, zolpidem causes a significant increase in $\tau_w$ of the averaged mIPSC in both C57BL/6 (pre = 4.37 ± 0.19ms, post = 6.80 ± 0.28ms, $n = 9$; $p < 0.0001$) and Thy1α6 mice (pre = 4.94 ± 0.55ms, post = 7.39 ± 0.15ms, $n = 7$; $p < 0.01$) (Fig. 10E–G). The percentage change in peak amplitude and $\tau_w$ following zolpidem application between C57BL/6 and Thy1α6 mice, however, is not significantly different for either measure (peak amplitude, C57BL/6 = 108.65 ± 4.9%; Thy1α6 = 117.78 ± 8.44%; $p > 0.1$; $\tau_w$,C57BL/6 = 157.48 ± 8.57%;Thy1α6 = 160.11 ± 16.29%; $p > 0.5$; $n = 9$ vs. 7 for both) (Fig. 10H). Thus, the effect of zolpidem is similar between C57BL/6 and Thy1α6 mice.

As a further test for the presence of $GABA_A$ receptors with α6 subunits in the synapse we looked at the furosemide response. Furosemide selectively antagonizes α4 and α6 subunit-containing receptors in the configuration α4/6β2/3γ2 and can be used to probe for these receptor subtypes (Korpi et al., 1995; Knoflach et al., 1996; Wafford et al., 1996; Korpi and Lüddens, 1997). We tested if the effects of furosemide on mIPSCs in CA1 pyramidal cells are different in Thy1α6 compared with C57BL/6 wild-type mice. Bath application of furosemide (600 μM) causes little change in the frequency of mIPSCs in either mouse strain (C57BL/6, pre − furosemide = 10.46 ± 1.80Hz, post − furosemide = 9.60 ± 1.45Hz, $n = 5$; $p > 0.1$; Thy1α6, pre = 11.76 ± 3.54Hz, post = 11.94 ± 3.21Hz, $n = 5$; $p > 0.5$). However, furosemide produces a small decrease in the peak amplitude of the averaged mIPSC in Thy1α6 (pre = −25.67 ± 2.72pA, post = −19.46 ± 1.07pA, $n = 5$; $p < 0.05$), but not wild-type C57BL/6 mice (pre = −39.35 ± 1.92pA, post = −34.34 ± 3.69pA, $n = 5$; $p > 0.1$) (Fig. 10A and B). Furosemide also significantly increased $\tau_w$ in both C57BL/6 (pre = 4.78 ± 0.36ms, post = 6.07 ± 0.56pA, $n = 5$; $p < 0.05$) and Thy1α6 mice (pre = 4.87 ± 0.26pA, post = 5.36 ± 0.20pA, $n = 5$; $p < 0.05$) (Fig. 10A and C). There was no significant difference in the decrease in peak amplitude and increase in $\tau_w$ of the averaged mIPSCs between C57BL/6 and Thy1α6 mice, as determined by calculating the changes as percentage of the pre-furosemide values (peak amplitude, C57BL/6 = 87.65 ± 9.52%; Thy1α6 = 77.64 ± 4.63%; $p > 0.1$; $\tau_w$, C57BL/6 = 126.94 ± 6.91%; Thy1α6 = 110.72 ± 3.96; $p > 0.05$; $n = 5$ vs. 5 for both) (Fig. 10D). Reducing furosemide concentration from 600 to 60 μM had little effect on the properties of the averaged mIPSCs in either C57BL/6 or Thy1α6 mice (both $n = 3$).

The zolpidem and furosemide data show that the synaptic $GABA_A$ receptors containing the α6 subunit, if present, are not significant relative to the normal synaptic receptor complement.

## 4. Discussion

During evolution the $GABA_A$ receptor α6 subunit has remained selectively associated with cerebellar granule cells and their homologues (Lüddens et al., 1990; Bahn et al., 1996; Hadingham et al., 1996; Campos et al., 2001; Varecka et al., 1994). In these cells the α6 subunit contributes to receptor types associated with extrasynaptic (tonic) inhibition (Brickley et al., 2001), as well as synaptic receptors (Nusser et al., 1996a,b; Mellor et al., 2000). This remarkably tight conservation of α6 expression suggests that tonic inhibition is important. In fact, in rodent granule cells, 90% of $GABA_A$ receptor-mediated the charge transfer is through the tonic current (Brickley et al., 2001). On the premise that misex-

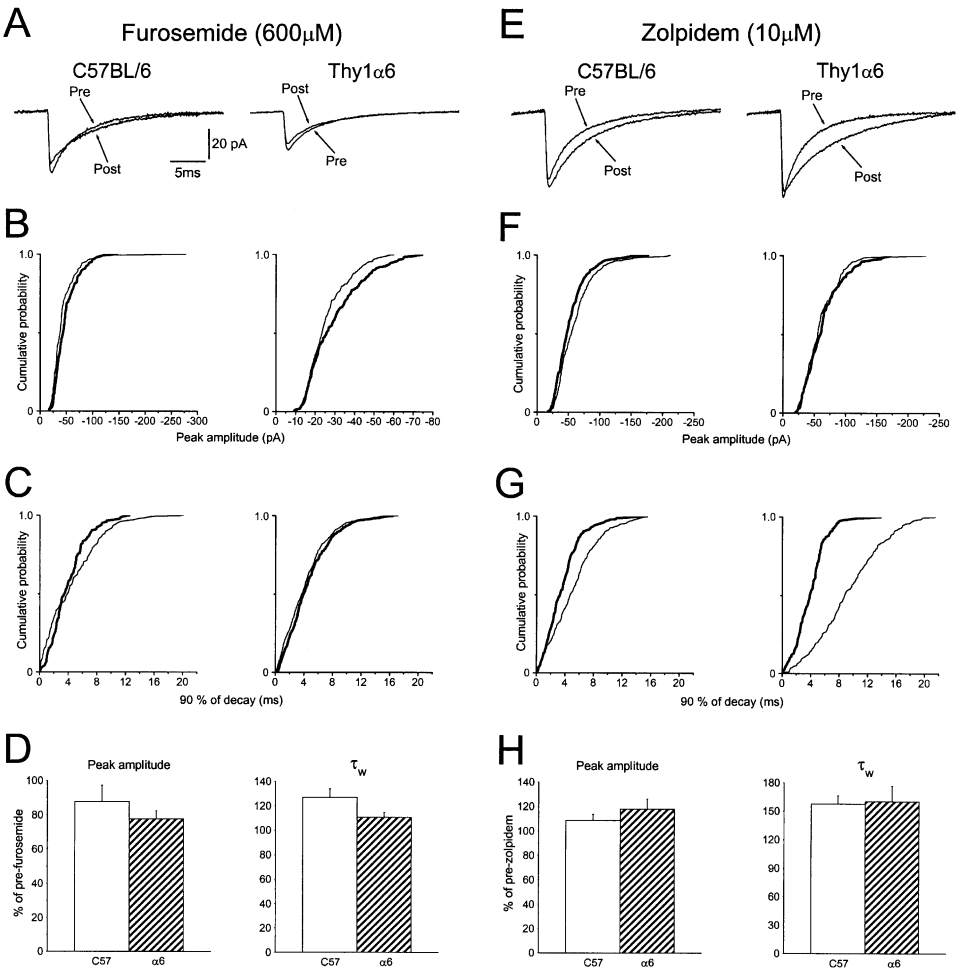


Fig. 10. Effects of furosemide and zolpidem on mIPSCs recorded from CA1 pyramidal cells of C57BL/6 and Thy1α6 mice. A. Comparison of effects of furosemide (600 μM) on the waveform of the averaged mIPSC recorded from a CA1 pyramidal cell of a C57BL/6 mouse (left) and a Thy1α6 mouse (right) in the presence of kynurenic acid (3 mM) and TTX (1 μM). B. Cumulative probability graphs of the effect of furosemide on peak amplitude for the cells shown in A. Thicker line represents pre-furosemide, thinner line post-furosemide (C57BL/6, pre-furosemide, $n = 145$ individual mIPSCs, post-furosemide, $n = 145$; Thy1α6, pre-furosemide, $n = 324$ individual mIPSCs, post-furosemide, $n = 308$). The effect of furosemide for both these cells is to cause a slight shift up and to the left, indicating a decrease in peak amplitude. C. Cumulative probability graphs of the effects of furosemide on time taken to reach 90% of decay, for the same cells as in A (*n* of individual mIPSCs as in B). Furosemide causes a shift down and to the right (left), indicating an increase in time to decay, or has no effect (right). D. Comparison of effects of furosemide on peak amplitude and $\tau_w$ between mouse strains. E. Comparison of effects of zolpidem (10 μM) on the waveform of the averaged mIPSC recorded from different CA1 pyramidal cells of a C57BL/6 mouse (left) and a Thy1α6 mouse (right) in the presence of kynurenic acid (3 mM) and TTX (1 μM). F. Cumulative probability graphs depicting the effect of zolpidem on the same cells as in E. Thicker line represents pre-zolpidem, thinner line post-zolpidem (C57BL/6, pre-zolpidem, $n = 280$ individual mIPSCs, post-zolpidem 300; Thy1α6, pre-zolpidem, $n = 202$ individual mIPSCs, post-zolpidem, $n = 205$). Note that there is little effect of zolpidem on peak amplitude for both cells. G. Cumulative probability graphs of the effect of zolpidem on the time to reach 90% of decay for the same cells as in E (*n* of individual mIPSCs as in F). The effect of zolpidem on time to decay is clearly a shift down and to the right as the result of a large increase in the decay time for both cells. H. Comparison of effects of zolpidem on peak amplitude and $\tau_w$ between mouse strains. Values in D and H are depicted as the percentage of the pre-drug mean for each mouse strain. Calibration bars in A also apply to E.

pression studies can sometimes be revealing for protein function, we took the α6 subunit out of its natural granule cell environment and ectopically expressed it in other neuronal types. The results reveal a strong apparent conservation of function. The α6 subunits expressed in forebrain neurons in Thy1α6 mice form α6βγ2, α1α6βγ2 and α3α6βγ2 receptors, which are largely extrasynaptic on cortical and CA1 pyramidal cells. Consistent with this subcellular location, Thy1α6 CA1 pyramidal neurons have a five-fold increased tonic $GABA_A$ receptor-mediated current compared with wild-type cells. The activation of these extrasynaptic receptors is probably mediated by ambient GABA spilling over from synaptic clefts since tonic currents on the CA1 pyramidal cells can only be detected by blocking the GABA uptake transporter GAT-1 (Frahm et al., 2001).

In Thy1α6 mice, most forebrain-expressed α6 immunoreactivity accumulates outside synaptic junctions. In

agreement with immunocytochemical data, there was little electrophysiological evidence for α6-containing $GABA_A$ receptors in the CA1 pyramidal cell synapse. Pharmacologically, the synaptic receptor populations were largely α1βγ2 both in Thy1α6 and C57BL/6 mice, since the α6 subunit-selective antagonist furosemide had no greater effects on spontaneous IPSCs in Thy1α6 than C57BL/6 mice, and the α1 subunit-preferring benzodiazepine agonist zolpidem had similar effects on mIPSCs in both lines. Overall, the subcellular distribution of the α6 subunit in isocortex layer V pyramidal cells and the hippocampal CA1 pyramidal cells in Thy1α6 mice resembles the subcellular distribution of the native α6 subunit in cerebellar granule cells of wild-type rodents, in as much as the α6 subunit is in the extrasynaptic membrane of dendrites and less frequently in type II (GABAergic) synapses (Nusser et al., 1996a,b, 1998, 1999). Due to the rare occurrence of forebrain synaptic labeling for the α6 subunit we did not attempt to quantify the proportion of labeled synapses. Both immunogold methods may underestimate synaptic labeling: the pre-embedding method is limited by antibody penetration; and the postembedding method may have limited sensitivity. Nevertheless, based on the immunofluorescence results it is likely that most surface transgenic α6 subunit-containing receptors are in the extrasynaptic membrane.

The strong labeling of the extrasynaptic membrane of dendritic spines with the α6 subunit-specific antibody was unexpected because spines rarely receive GABAergic innervation (Megias et al., 2001). Perhaps the transgenic expression of the α6 subunit triggers $GABA_A$ receptor targeting to dendritic spines; or the incorporation of the α6 subunit reveals the normally high level of spine $GABA_A$ receptors, which has not previously been detected through lack of suitable antibodies. For example, the precise subcellular location of α5 or α4 subunit-containing $GABA_A$ receptors on the pyramidal cell surface in vivo is not known and these subunits may be present on the extrasynaptic membrane of dendritic spines. In fact, in hippocampal pyramidal neurons, the α5 subunit seems largely extrasynaptic (Brünig et al., 2002; Crestani et al., 2002).

From ligand binding and protein immunopurification, the α6 subunits in the Thy1α6 forebrain are mainly incorporated into α6βγ2 receptors and some also exist as α1α6βγ2 and α3α6βγ2 receptors. In cerebellar granule cells, many of the α6 receptor subunits are likely located in the synapse, probably in receptors consisting of α6β2/3γ2 and/or α1α6βγ2 subunits (Somogyi et al., 1996; Nusser et al., 1996a,b, 1999; Pollard et al., 1995; Khan et al., 1996; Jechlinger et al., 1998; Sigel and Baur, 2000; reviewed in Wisden and Farrant, 2002). In both forebrain and cerebellar synapses the γ2 subunit is believed essential for either bringing the receptors into the synapse or tethering them there, probably via binding proteins such as gephyrin (Essrich et al., 1998; Kneussel et al., 1999; Moss and Smart, 2001). However, the γ2 subunit cannot be the sole factor for synaptic targeting because otherwise significant numbers of α6 subunits would be synaptically located in forebrain neurons of Thy1α6 mice. Thus, there must be some influence from the α subunit type and an interaction with the γ2 subunit in order to get synaptically targeted receptors (Kneussel et al., 2001).

In cerebellar granule cells, the α6βδ combination is prominent (Jones et al., 1997; Nusser et al., 1999). Why are no α6βδ receptors formed, at least to any great extent, in the forebrain of Thy1α6 mice? The α4 and α6 subunits are probably paralogues with similar functions; and in some neurons (e.g., those in thalamus and dentate granule cells) α6βδ-containing receptors may form receptors that sense extrasynaptic GABA (Sur et al., 1999; Korpi et al., 2002; Nusser and Mody, 2002; Peng et al., 2002). In Thy1α6 forebrain neurons, the α4 subunit may out-compete the α6 subunit during receptor subunit assembly because in absolute terms δ prefers α4 to α6. Alternatively, and more probably, the lack of α6βδ receptors is not surprising as Thy1α6 transgene expression does not substantially overlap with native δ subunit gene expression—perhaps the only strong overlap being the dentate granule cells—and the resulting α6βδ receptors formed in these cells would be at a too low concentration to be detectable in total forebrain extract. There is little detectable δ subunit mRNA or immunoreactivity in CA1 pyramidal cells (Shivers et al., 1989; Wisden et al., 1992; Fritschy and Möhler, 1995; Pirker et al., 2000; Sperk et al., 1997; Peng et al., 2002).

It seems likely that tonic currents can be generated by different α6 receptor subunit combinations and even different $GABA_A$ receptor subtypes. For example, GABA receptors formed from ρ subunits are well adapted for a 'tonic role', forming non-desensitizing channels which give small currents (Zhang et al., 2001). In cerebellar granule cells recorded in tissue slices the tonic current is from α6βδ receptors (Brickley et al., 2001; Hamman et al., 2002); but in the presence of benzodiazepine agonists, extrasynaptic α1βγ2 receptors probably also contribute (Leao et al., 2000). In this case the affinity of α1βγ2 receptors for GABA is substantially increased by benzodiazepines, enabling them to respond to ambient extrasynaptic GABA. In Thy1α6 CA1 pyramidal cells, given the paucity of native δ subunit expression, the extrasynaptic current, we detect probably originates from either α6βγ2 or α1α6βγ2 receptors.

The functions of background conductances in neuronal circuits are unknown. Small and persistent (tonic) chloride conductances alter input resistance and membrane time constants; these in turn influence synaptic efficacy and integration (reviewed in Bai et al., 2001; De Schutter, 2002). For example, in cerebellar granule cells tonic inhibition via α6δ subunit-containing $GABA_A$

receptors could constrain coincidence detection from mossy fiber inputs, so that only closely timed excitatory inputs excite the cell to fire an action potential (Brickley et al., 2001; Hamann et al., 2002; De Schutter, 2002). Manipulating background inhibitory currents can probably influence epileptic thresholds. The Thy1α6 mice described here will be useful for studying the contributions and influences of background $GABA_A$-receptor-mediated currents in inhibiting seizures (Cheng et al., 2001).

One further difference between the Thy1α6 and wild-type mice is worth comment. The significantly lower frequency of spontaneous IPSCs in Thy1α6 mice compared with C57BL/6 mice may result from a compensatory mechanism. A lower frequency of events was a trend for both spontaneous IPSCs recorded in the presence of NO-711, and mIPSCs. In addition, the peak amplitude of the mIPSCs was significantly lower in Thy1α6 mice compared with the C57BL/6 strain and there was a trend for smaller peak amplitude of the averaged spontaneous IPSCs in Thy1α6 mice compared with those in C57BL/6 mice. One possible explanation is that the larger tonic current in the Thy1α6 mice, resulting in a greater level of baseline noise, masks small IPSCs/mIPSCs, thereby reducing their frequency. However, the smallest individual mIPSCs were consistently smaller in Thy1α6 mice compared with C57BL/6 mice; therefore, this scenario is unlikely. It is also possible that expression of the α6 subunit in GABAergic interneurones could reduce their excitability and so reduce the frequency of IPSCs in pyramidal cells, but his could not explain the lower amplitude of mIPSCs. Therefore, the fascinating possibility remains that pyramidal cells activate intrinsic compensatory mechanisms, which, in response to the increased extrasynaptic tonic current, reduce the effects of synaptic $GABA_A$-receptor-mediated inhibition. In cerebellar granule cells, genetic disruption of the α6 subunit results in a subsequent compensatory increase in a $K^+$ 'leak' conductance, so that overall levels of tonic current are maintained (Brickley et al., 2001). Here, in the Thy1α6 mice, $GABA_A$ receptor-implemented homeostatic mechanisms could be envisaged, as is observed for $GABA_A$ receptor adaptations during benzodiazepine tolerance or in response to steroids (Arnot et al., 2001; Brussaard and Herbison, 2000; Gulinello et al., 2001; Smith et al., 1998).

## Acknowledgements

This work was supported by the Medical Research Council (P.S. and W.W.), EC Project ERBBI-O4CT960585 (W.S. and P.S.), the Austrian Ministry for Science and Traffic, Nr. GZ 70.077/1-Pr/4/2000 (W.S.); the Austrian Science Fund, project P14385-Gen (W.S.); NIH grant NS35985 (I.M.); the Academy of Finland (E.R.K.); and Deutsche Forschungsgemeinschaft WI 1951/1-1 (WW). We thank Mark Farrant (UCL, London) and Francesco Ferraguti (MRC, Oxford) for discussion; Stephen Moss (UCL, London) for the Flagα6 cDNA; Zoltan Nusser (Inst. Exp. Medicine, Hungary) for helpful comments on the manuscript; Michel Goedert (MRC LMB, Cambridge) for drawing our attention to the Thy-1.2 expression cassette; Theresa Langford (MRC LMB, Cambridge) and Franceso Ferraguti (MRC Oxford) for substantial help with mouse logistics; and Philip Cobden, Paul Jays and David Roberts (all MRC Oxford) for excellent assistance with histology.

## References

Arnot, M.I., Davies, M., Martin, I.L., Bateson, A.N., 2001. $GABA_A$ receptor gene expression in rat cortex: differential effects of two chronic diazepam treatment regimes. Journal of Neuroscience Research 64, 617–625.

Bahn, S., Harvey, R.J., Darlison, M.G., Wisden, W., 1996. Conservation of γ-aminobutyric acid type A receptor α6 subunit gene expression in cerebellar granule cells. Journal of Neurochemistry 66, 1810–1818.

Bai, D., Zhu, G., Pennefather, P., Jackson, M.F., MacDonald, J.F., Orser, B.A., 2001. Distinct functional and pharmacological properties of tonic and quantal inhibitory postsynaptic currents mediated by γ-aminobutyric acid(A) receptors in hippocampal neurons. Molecular Pharmacology 59, 814–824.

Banks, M.I., Pearce, R.A., 2000. Kinetic differences between synaptic and extrasynaptic $GABA_A$ receptors in CA1 pyramidal cells. Journal of Neuroscience 20, 937–948.

Barnard, E.A., Skolnick, P., Olsen, R.W., Möhler, H., Sieghart, W., Biggio, G., Braestrup, C., Bateson, A.N., Langer, S.Z., 1998. International Union of Pharmacology, XV. Subtypes of γ-aminobutyric acid A receptors: classification on the basis of subunit structure and receptor function. Pharmacological Reviews 50, 291–313.

Baude, A., Nusser, Z., Roberts, J.D., Mulvihill, E., McIlhinney, R.A., Somogyi, P., 1993. The metabotropic glutamate receptor (mGluR1α) is concentrated at perisynaptic membrane of neuronal subpopulations as detected by immunogold reaction. Neuron 11, 771–787.

Borden, L.A., Murali Dhar, T.G., Smith, K.E., Weinshank, R.L., Branchek, T.A., Gluchowski, C., 1994. Tiagabine, SK&F 89976-A, CI-966 and NNC-711 are selective for the cloned GABA transporter GAT-1. European Journal of Pharmacology 269, 219–224.

Brickley, S.G., Cull-Candy, S.G., Farrant, M., 1996. Development of a tonic form of synaptic inhibition in rat cerebellar granule cells resulting from persistent activation of $GABA_A$ receptors. Journal of Physiology 497, 753–759.

Brickley, S.G., Cull-Candy, S.G., Farrant, M., 1999. Single-channel properties of synaptic and extrasynaptic $GABA_A$ receptors suggest differential targeting of receptor subtypes. Journal of Neuroscience 19, 2960–2973.

Brickley, S.G., Revilla, V., Cull-Candy, S.G., Wisden, W., Farrant, M., 2001. Adaptive regulation of neuronal excitability by a voltage-independent potassium conductance. Nature 409, 88–92.

Brünig, I., Scotti, E., Sidler, C., Fritschy, J.M., 2002. Intact sorting, targeting, and clustering of γ-aminobutyric acid A receptor subtypes in hippocampal neurons in vitro. Journal of Comparative Neurology 443, 43–55.

Brussaard, A.B., Herbison, A.E., 2000. Long-term plasticity of postsynaptic $GABA_A$-receptor function in the adult brain: insights from the oxytocin neurone. Trends in Neuroscience 23, 190–195.

Campos, M.L., de Cabo, C., Wisden, W., Juiz, J.M., Merlo, D., 2001. Expression of $GABA_A$ receptor subunits in rat brainstem auditory pathways: cochlear nuclei, superior olivary complex and nucleus of the lateral lemniscus. Neuroscience 102, 625–638.

Caroni, P., 1997. Overexpression of growth-associated proteins in the neurons of adult transgenic mice. Journal of Neuroscience Methods 71, 3–9.

Cheng, Q., Kulli, J.C., Yang, J., 2001. Suppression of neuronal hyperexcitability and associated delayed neuronal death by adenoviral expression of $GABA_C$ receptors. Journal of Neuroscience 21, 3419–3428.

Crestani, F., Keist, R., Fritschy, J.-M., Benke, D., Vogt, K., Pruts, L., Blüthmann, H., Möhler, H., Rudolph, U., 2002. Trace fear conditioning involves hippocampal α5 $GABA_A$ receptors. Proceedings of the National Academy of Sciences, USA 99, 8980–8985.

De Schutter, E., 2002. Cerebellar cortex: computation by extrasynaptic inhibition? Current Biology 12, R363–R365.

Essrich, C., Lorez, M., Benson, J.A., Fritschy, J.M., Luscher, B., 1998. Postsynaptic clustering of major $GABA_A$ receptor subtypes requires the γ2 subunit and gephyrin. Nature Neuroscience 1, 563–571.

Frahm, C., Engel, D., Draguhn, A., 2001. Efficacy of background GABA uptake in rat hippocampal slices. Neuroreport 12, 1593–1596.

Fritschy, J.-M., Möhler, H., 1995. $GABA_A$-receptor heterogeneity in the adult rat brain: differential regional and cellular distribution of seven major subunits. The Journal of Comparative Neurology 359, 154–194.

Gulinello, M., Gong, Q.H., Li, X., Smith, S.S., 2001. Short-term exposure to a neuroactive steroid increases α4 $GABA_A$ receptor subunit levels in association with increased anxiety in the female rat. Brain Research 910, 55–66.

Haas, K.F., Macdonald, R.L., 1999. $GABA_A$ receptor subunit γ2 and δ subtypes confer unique kinetic properties on recombinant $GABA_A$ receptor currents in mouse fibroblasts. Journal of Physiology 514, 27–45.

Hadingham, K.L., Garrett, E.M., Wafford, K.A., Bain, C., Heavens, R.P., Sirinathsinghji, D.J.S., Whiting, P.J., 1996. Cloning of cDNAs encoding the human γ-aminobutyric acid type A receptor α6 subunit and characterization of the pharmacology of α6-containing receptors. Molecular Pharmacology 49, 253–259.

Hamann, M., Rossi, D.J., Attwell, D., 2002. Tonic and spillover inhibition of granule cells control information flow through cerebellar cortex. Neuron 33, 625–633.

Hevers, W., Lüddens, H., 1998. The diversity of $GABA_A$ receptors. Pharmacological and electrophysiological properties of $GABA_A$ channel subtypes. Molecular Neurobiology 18, 35–86.

Hevers, W., Lüddens, H., 2002. Pharmacological heterogeneity of γ-aminobutyric acid receptors during development suggests distinct classes of rat cerebellar granule cells in situ. Neuropharmacology 42, 34–47.

Hevers, W., Korpi, E.R., Lüddens, H., 2000. Assembly of functional α6β3γ2δ $GABA_A$ receptors in vitro. Neuroreport 11, 4103–4106.

Hogan, B., Beddington, R., Constantini, F., Lacy, E., 1994. Manipulating the mouse embryo: a laboratory manual. Cold Spring Harbor Laboratory Press, New York.

Ichinose, T., Lukasiewicz, P.D., 2002. GABA transporters regulate inhibition in the retina by limiting $GABA_C$ receptor activation. Journal of Neuroscience 22, 3285–3292.

Jechlinger, M., Pelz, R., Tretter, V., Klausberger, T., Sieghart, W., 1998. Subunit composition and quantitative importance of heterooligomeric receptors: $GABA_A$ receptors containing α6 subunits. Journal of Neuroscience 18, 2449–2457.

Jensen, K., Mody, I., 2001. GHB depresses fast excitatory and inhibitory synaptic transmission via $GABA_B$ receptors in mouse neocortical neurons. Cerebral Cortex 11, 424–429.

Jones, A., Bahn, S., Grant, A.L., Köhler, M., Wisden, W., 1996. Characterization of a cerebellar granule cell-specific gene encoding the γ-aminobutyric acid type A receptor α6 subunit. Journal of Neurochemistry 67, 907–916.

Jones, A., Korpi, E.R., McKernan, R.M., Pelz, R., Nusser, Z., Makela, R., Mellor, J.R., Pollard, S., Bahn, S., Stephenson, F.A., Randall, A.D., Sieghart, W., Somogyi, P., Smith, A.J.H., Wisden, W., 1997. Ligand-gated ion channel subunit partnerships: $GABA_A$ receptor α6 subunit gene inactivation inhibits δ subunit expression. Journal of Neuroscience 17, 1350–1362.

Kaneda, M., Farrant, M., Cull-Candy, S.G., 1995. Whole-cell and single-channel currents activated by GABA and glycine in granule cells of the rat cerebellum. Journal of Physiology 485, 419–435.

Khan, Z.U., Gutiérrez, A., DeBlas, A.L., 1996. The α1 and α6 subunits can coexist in the same cerebellar $GABA_A$ receptor maintaining their individual benzodiazepine-binding specificities. Journal of Neurochemistry 66, 685–691.

Klausberger, T., Roberts, J.D., Somogyi, P., 2002. Cell type- and input-specific differences in the number and subtypes of synaptic $GABA_A$ receptors in the hippocampus. Journal of Neuroscience 22, 2513–2521.

Kneussel, M., Brandstätter, J.H., Laube, B., Stahl, S., Müller, U., Betz, H., 1999. Loss of postsynaptic $GABA_A$ receptor clustering in gephyrin-deficient mice. Journal of Neuroscience 19, 9289–9297.

Kneussel, M., Brandstätter, J.H., Gasnier, B., Feng, G., Sanes, J.R., Betz, H., 2001. Gephyrin-independent clustering of postsynaptic $GABA_A$ receptor subtypes. Molecular and Cellular Neuroscience 17, 973–982.

Knoflach, F., Benke, D., Wang, Y., Scheurer, L., Lüddens, H., Hamilton, B.J., Carter, D.B., Möhler, H., Benson, J.A., 1996. Pharmacological modulation of the diazepam-insensitive recombinant γ-aminobutyric acidA receptors α4β2γ2 and α6β2γ2. Molecular Pharmacology 50, 1253–1261.

Korpi, E.R., Lüddens, H., 1997. Furosemide interactions with brain $GABA_A$ receptors. British Journal of Pharmacology 120, 741–748.

Korpi, E.R., Kuner, T., Seeburg, P.H., Lüddens, H., 1995. Selective antagonist for the cerebellar granule cell-specific γ-aminobutyric acid type A receptor. Molecular Pharmacology 47, 283–289.

Korpi, E.R., Koikkalainen, P., Vekovischeva, O.Y., Makela, R., Kleinz, R., Uusi-Oukari, M., Wisden, W., 1999. Cerebellar granule-cell-specific $GABA_A$ receptors attenuate benzodiazepine-induced ataxia: evidence from α6-subunit-deficient mice. European Journal of Neuroscience 11, 233–240.

Korpi, E.R., Mihalek, R.M., Sinkkonen, S.T., Hauer, B., Hevers, W., Homanics, G.E., Sieghart, W., Lüddens, H., 2002. Altered receptor subtypes in the forebrain of $GABA_A$ receptor δ subunit-deficient mice: recruitment of γ2 subunits. Neuroscience 109, 733–743.

Landsend, A.S., Amiry-Moghaddam, M., Matsubara, A., Bergersen, L., Usami, S., Wenthold, R.J., Ottersen, O.P., 1997. Differential localization of δ glutamate receptors in the rat cerebellum: coexpression with AMPA receptors in parallel fiber-spine synapses and absence from climbing fiber-spine synapses. Journal of Neuroscience 17, 834–842.

Leao, R.M., Mellor, J.R., Randall, A.D., 2000. Tonic benzodiazepine-sensitive GABAergic inhibition in cultured rodent cerebellar granule cells. Neuropharmacology 39, 990–1003.

Lüddens, H., Pritchett, D.B., Köhler, M., Killisch, I., Keinänen, K., Monyer, H., Sprengel, R., Seeburg, P.H., 1990. Cerebellar $GABA_A$ receptor selective for a behavioural alcohol antagonist. Nature 346, 648–651.

Mäkelä, R., Uusi-Oukari, M., Homanics, G.E., Quinlan, J.J., Firestone, L.L., Wisden, W., Korpi, E.R., 1997. Cerebellar γ-aminobutyric acid type A receptors: pharmacological subtypes revealed by mutant mouse lines. Molecular Pharmacology 52, 380–388.

Megias, M., Emri, Z., Freund, T.F., Gulyas, A.I., 2001. Total number and distribution of inhibitory and excitatory synapses on hippocampal CA1 pyramidal cells. Neuroscience 102, 527–540.

Mellor, J.R., Wisden, W., Randall, A.D., 2000. Somato-synaptic vari-

ation of $GABA_A$ receptors in cultured murine cerebellar granule cells: investigation of the role of the α6 subunit. Neuropharmacology 39, 1495–1513.

Mitchell, S.J., Silver, R.A., 2000. GABA spillover from single inhibitory axons suppresses low-frequency excitatory transmission at the cerebellar glomerulus. Journal of Neuroscience 20, 8651–8658.

Mody, I., 2001. Distinguishing between $GABA_A$ receptors responsible for tonic and phasic conductances. Neurochemical Research 26, 907–913.

Moss, S.J., Smart, T.G., 2001. Constructing inhibitory synapses. Nature Reviews Neuroscience 2, 240–250.

Mossier, B., Tögel, M., Fuchs, K., Sieghart, W., 1994. Immunoaffinity purification of γ-aminobutyric acid $_A$ ($GABA_A$) receptors containing γ1 subunits. Journal of Biological Chemistry 269, 25777–25782.

Nusser, Z., Mody, I., 2002. Selective modulation of tonic and phasic inhibitions in dentate gyrus granule cells. Journal of Neurophysiology 87, 2624–2628.

Nusser, Z., Sieghart, W., Benke, D., Fritschy, J.M., Somogyi, P., 1996a. Differential synaptic localization of two major γ-aminobutyric acid type A receptor α subunits on hippocampal pyramidal cells. Proceedings of the National Academy of Science, USA 93, 11939–11944.

Nusser, Z., Sieghart, W., Stephenson, F.A., Somogyi, P., 1996b. The α6 subunit of the $GABA_A$ receptor is concentrated in both inhibitory and excitatory synapses on cerebellar granule cells. Journal of Neuroscience 16, 103–114.

Nusser, Z., Sieghart, W., Somogyi, P., 1998. Segregation of different $GABA_A$ receptors to synaptic and extrasynaptic membranes of cerebellar granule cells. Journal of Neuroscience 18, 1693–1703.

Nusser, Z., Ahmad, Z., Tretter, V., Fuchs, K., Wisden, W., Sieghart, W., Somogyi, P., 1999. Alterations in the expression of $GABA_A$ receptor subunits in cerebellar granule cells after the disruption of the α6 subunit gene. European Journal of Neuroscience 11, 1685–1697.

Nyiri, G., Freund, T.F., Somogyi, P., 2001. Input-dependent synaptic targeting of α2 subunit-containing $GABA_A$ receptors in synapses of hippocampal pyramidal cells of the rat. European Journal of Neuroscience 13, 428–442.

Otis, T.S., Staley, J., Mody, I., 1991. Perpetual inhibitory activity in mammalian brain slices generated by spontaneous GABA release. Brain Research 545, 142–150.

Peng, Z., Hauer, B., Mihalek, R.M., Homanics, G.E., Sieghart, W., Olsen, R.W., Houser, C.R., 2002. $GABA_A$ receptor changes in δ subunit-deficient mice: altered expression of α4 and γ2 subunits in the forebrain. Journal of Comparative Neurology 446, 179–197.

Pirker, S., Schwarzer, C., Wieselthaler, A., Sieghart, W., Sperk, G., 2000. $GABA_A$ receptors: immunocytochemical distribution of 13 subunits in the adult rat brain. Neuroscience 101, 815–850.

Pollard, S., Thompson, C.L., Stephenson, F.A., 1995. Quantitative characterization of α6 and α1α6 subunit-containing native γ-aminobutyric $acid_A$ receptors of adult rat cerebellum demonstrates two α subunits per receptor oligomer. Journal of Biological Chemistry 270, 21285–21290.

Rossi, D.J., Hamann, M., 1998. Spillover-mediated transmission at inhibitory synapses promoted by high affinity α6 subunit $GABA_A$ receptors and glomerular geometry. Neuron 20, 783–795.

Saxena, N.C., Macdonald, R.L., 1996. Properties of putative cerebellar gamma-aminobutyric acid A receptor isoforms. Molecular Pharmacology 49, 567–579.

Shivers, B.D., Killisch, I., Sprengel, R., Sontheimer, H., Köhler, M., Schofield, P.R., Seeburg, P.H., 1989. Two novel $GABA_A$ receptor subunits exist in distinct neuronal subpopulations. Neuron 3, 327–337.

Sigel, E., Baur, R., 2000. Electrophysiological evidence for the coexistence of α1 and α6 subunits in a single functional $GABA_A$ receptor. Journal of Neurochemistry 74, 2590–2596.

Smith, S.S., Gong, Q.H., Li, X., Moran, M.H., Bitran, D., Frye, C.A., Hsu, F.C., 1998. Withdrawal from 3α-OH-5α-pregnan-20-One using a pseudopregnancy model alters the kinetics of hippocampal $GABA_A$-gated current and increases the $GABA_A$ receptor α4 subunit in association with increased anxiety. Journal of Neuroscience 18, 5275–5284.

Somogyi, P., Fritschy, J.-M., Benke, D., Roberts, J.D.B., Sieghart, W., 1996. The γ2 subunit of the $GABA_A$ receptor is concentrated in synaptic junctions containing the α1 and β2/3 subunits in hippocampus, cerebellum and globus pallidus. Neuropharmacology 35, 1425–1444.

Somogyi, P., Tamas, G., Lujan, R., Buhl, E.H., 1998. Salient features of synaptic organisation in the cerebral cortex. Brain Research Reviews 26, 113–135.

Sperk, G., Schwarzer, C., Tsunashima, K., Fuchs, K., Sieghart, W., 1997. $GABA_A$ receptor subunits in the rat hippocampus I: immunocytochemical distribution of 13 subunits. Neuroscience 80, 987–1000.

Sur, C., Farrar, S.J., Kerby, J., Whiting, P.J., Atack, J.R., McKernan, R.M., 1999. Preferential coassembly of α4 and δ subunits of the γ-aminobutyric acidA receptor in rat thalamus. Molecular Pharmacology 56, 110–115.

Tia, S., Wang, J.F., Kotchabhakdi, N., Vicini, S., 1996. Developmental changes of inhibitory synaptic currents in cerebellar granule neurons: role of $GABA_A$ receptor α6 subunit. Journal of Neuroscience 16, 3630–3640.

Tögel, M., Mossier, B., Fuchs, K., Sieghart, W., 1994. γ-Aminobutyric $acid_A$ receptors displaying association of $\gamma_3$-subunits with $\beta_{2/3}$ and different α-subunits exhibit unique pharmacological properties. Journal of Biological Chemistry 269, 12993–12998.

Tretter, V., Ehya, N., Fuchs, K., Sieghart, W., 1997. Stoichiometry and assembly of a recombinant $GABA_A$ receptor subtype. Journal of Neuroscience 17, 2728–2737.

Tretter, V., Hauer, B., Nusser, Z., Mihalek, R.M., Hoger, H., Homanics, G.E., Somogyi, P., Sieghart, W., 2001. Targeted disruption of the $GABA_A$ receptor δ subunit gene leads to an up-regulation of γ2 subunit-containing receptors in cerebellar granule cells. Journal of Biological Chemistry 276, 10532–10538.

Varecka, L., Wu, C.-H., Rotter, A., Frostholm, A., 1994. $GABA_A$/benzodiazepine receptor α6 subunit mRNA in granule cells of the cerebellar cortex and cochlear nuclei: expression in developing and mutant mice. Journal of Comparative Neurology 339, 341–352.

Vicini, S., Ferguson, C., Prybylowski, K., Kralic, J., Morrow, A.L., Homanics, G.E., 2001. $GABA_A$ receptor α1 subunit deletion prevents developmental changes of inhibitory synaptic currents in cerebellar neurons. Journal of Neuroscience 21, 3009–3016.

Wafford, K.A., Thompson, S.A., Thomas, D., Sikela, J., Wilcox, A.S., Whiting, P.J., 1996. Functional characterization of human γ-aminobutyric acidA receptors containing the α4 subunit. Molecular Pharmacology 50, 670–678.

Wall, M.J., Usowicz, M.M., 1997. Development of action potential-dependent and independent spontaneous $GABA_A$ receptor-mediated currents in granule cells of postnatal rat cerebellum. European Journal of Neuroscience 9, 533–548.

Wisden, W., Laurie, D.J., Monyer, H., Seeburg, P.H., 1992. The distribution of 13 $GABA_A$ receptor subunit mRNAs in the rat brain, I. Telencephalon, diencephalon, mesencephalon. Journal of Neuroscience 12, 1040–1062.

Wisden, W., Farrant, M., 2002. Insights into $GABA_A$ receptor complexity from the study of cerebellar granule cells: synaptic and extrasynaptic receptors. In: Egebjerg, J., Schousboe, A., Krogsgaard-Larsen, P. (Eds.), Glutamate and GABA Receptors and Transporters: Structure, Function and Pharmacology. Taylor and Francis, London, pp. 189–201.

Wisden, W., Morris, B.J., 2002. In situ hybridization with oligonucleotide probes. In: Wisden, W., Morris, B.J. (Eds.), In Situ Hybridiz-

ation Protocols for the Brain, second ed. International Review of Neurobiology, vol. 47. Academic Press, London, pp. 4–59.

Zezula, J., Fuchs, K., Sieghart, W., 1991. Separation of α1, α2, and α3 subunits of the $GABA_A$-benzodiazepine receptor complex by immunoaffinity chromatography. Brain Research 563, 325–328.

Zhang, D., Pan, Z.H., Awobuluyi, M., Lipton, S.A., 2001. Structure and function of $GABA_C$ receptors: a comparison of native versus recombinant receptors. Trends in Pharmacological Sciences 22, 121–132.